Feeding behavior and functional morphology of the neck in the long-snouted aquatic fossil reptile *Champsosaurus* (Reptilia: Diapsida) in comparison with the modern crocodilian *Gavialis gangeticus*.

Ryoko Matsumoto[1] Shin-ichi Fujiwara[2] and Susan E. Evans[3]

1. Kanagawa Prefectural Museum of Natural History, 499 Iryuda, Odawara, Kanagawa 250-0031, Japan, r-matsumoto@nh.kanagawa-museum.jp*

2. The Nagoya University Museum, Furocho, Chikusa-ku, Nagoya 464-8601 JAPAN, sifjwr@num.nagoya-u.ac.jp

3. Centre for Integrative Anatomy, Department of Cell and Developmental Biology, UCL, University College London, Gower Street, London WC1E 6BT, United Kingdom, ucgasue@ucl.ac.uk

Abstract

The extinct freshwater choristoderan reptiles *Champsosaurus* and *Simoedosaurus* are characterised by a large body size and an elongated snout. They have often been considered as eco-analogues of crocodilians based on superficial similarities. The slender-snouted *Champsosaurus* has been described as a “gavial-like reptile”, which implies it feeds underwater with a lateral swipe of the head and neck, as in the living slender-snouted crocodilians such as *Gavialis gangeticus.* In contrast, the short-snouted *Simoedosaurus* is often compared with short-snouted living crocodilians, and is considered to take single prey items. However, the neck mobility and flexibility needed for feeding movements are poorly understood even in extant crocodilians. This study explores the relationship between cervical morphology and neck flexion, focusing particularly in lateral and dorsal movements in *G. gangeticus* by comparison with shorter-snouted crocodilians. The paper also describes a method to estimate the maximum angle of neck dorsi-flexion in

choristoderes, based on the cervical morphology of extant crocodilian species. Three Indices were used in this study, of which Index 3 is newly proposed, to compare cervical morphology and intervertebral joint flexibility: 1) Enclosed zygapophyseal angles (EZA) as an Index of dorso-ventral/ bilateral flexibility; 2) moment arm (M) of dorsi-flexor muscles as an Index of resistance against ventro-flexion; and 3) the orientations of zygapophysial facets for a maximum angle of dorsi-flexion. These Indices were validated using μCT scanning of fresh specimens of *G. gangeticus* and *Caiman latirostris* in lateral and dorsal flexion. A unique mechanism of lateral flexion was identified in *G. gangeticus* that uses a combination of the following features: 1) lateral flexion mainly restricted to the anterior cervical vertebrae (v2/v3: high EZA, with more horizontal zygapophyses); and 2) high degree of dorsi-flexion at the v3/v4 and v4/v5 joints with potential for dorsal flexibility through the middle-posterior neck, which is used in inertial feeding. In contrast, *Champsosaurus* and *Simoedosaurus* possess relatively short cervical vertebrae, as in short-snouted crocodilians. The middle-posterior cervical vertebrae of *Champsosaurus* are specialised for lateral flexion (high EZA), and there is only limited capacity for dorsi-flexion throughout the neck. Like *G. gangeticus*, therefore, *Champsosaurus* may have used its slender snout to grab fish from shoals using lateral sweeping motions of the head and neck, but the movement is through the neck not the cranio-cervical joint. However inertial feeding is less likely to have occurred in this genus, and the aligned palatal dentition may have aided lingual transport of prey into the mouth. *Simoedosaurus*, on the other hand, appears to have been less specialised, with a neck that combined lateral and dorsolateral flexion, a motion that could have been effective in catching both terrestrial and aquatic prey. Where these two choristoderan genera occurred in same place, they may have divided their niche by prey types.

Keywords: Neochoristodera, Cervical vertebrae, Platyrostral, Feeding behaviour, Crocodylia,

INTRODUCTION

Choristoderes were a primarily Laurasian clade of freshwater reptiles recorded from the Middle Jurassic (~166 million years ago [mya]) to the Miocene (~16 mya). Choristoderan monophyly is not disputed, but the phylogenetic position of the group within diapsids remains problematic. It is generally argued that choristoderes might lie either on the stem of diapsids (e.g. Dilkes 1998) or of archosauromorphs (e.g. Neenan et al. 2013). Choristoderes share a unique morphology, most notably in the depressed posterior part of the skull which appears cordiform (heart-shaped) in dorsal view (e.g. Evans & Hecht 1993; Matsumoto et al. 2013). However, research over the last three decades has revealed considerable disparity in the morphology of both the skull and body proportions, and in body size (small lizard-like type; long-necked type; large long-snouted type: e.g. Evans 1990; Evans & Manabe 1999; Gao et al. 2000; Matsumoto & Evans 2010).

The long-snouted choristoderan morphotype (Neochoristodera: Evans & Hecht 1993) is first recorded from in the Lower Cretaceous (~120 mya) of Asia. Neochoristoderes became widely distributed through Euramerica in the Upper Cretaceous, survived into the Paleocene, but then apparently became extinct. *Champsosaurus* (Upper Cretaceous to Eocene, ~94–47 mya) and *Simoedosaurus* (Paleocene–Early Eocene) are representative neochoristodere taxa (Fig. 1) characterised by relatively large body size (~2–5 m in total length: Matsumoto & Evans 2010).

Gans (1969) noted that animals feeding under water need to overcome the frictional resistance of a viscous medium. One of the structural solutions to this problem is to develop a long slender snout that reduces the sagittal cross-section of the snout and thus reduces the drag when the snout is swept horizontally about a centre located near the braincase or in the neck region (Gans 1969). Furthermore, elongation of the snout maximises the grasping arm for foraging. This structure and behaviour are well demonstrated in the extant piscivorous crocodilian *Gavialis gangeticus* (Fig. 1). While gavials forage under water, rapid lateral strikes are produced principally by the head and neck (Neill 1971; Thorbjarnarson 1990). These long-snouted (longirostrine) crocodilians, including *Gavialis gangeticus* and *Tomistoma schlegelii*, have a relatively lightly built cranium compared to

short-snouted crocodilians (Cleuren & De Vree 1992), reflecting the fact that their prey is generally small and requires rapid movement under water. Once the prey is captured, mainly in the middle third of the mouth, the head is lifted above the water and a holding and tossing motion is used to manipulate the prey into the mouth as in other crocodilians (inertial feeding; Gans 1969). In contrast, short-snouted crocodilians including *Alligator mississippiensis* tend to have strongly built skulls (Cleuren & De Vree 1992), allowing them to hold large prey in their jaws. The prey can be dismembered by spinning the head-neck, body and tail (Pooley & Gans 1976; Taylor 1987; Fish et al. 2007), an action that also involves the axial skeleton. A recent comparative study of presacral vertebrae in extant crocodilians (Iijima & Kubo 2019) highlighted differences in neck morphology between *Gavialis gangeticus* and other crocodilians that may reflect the differences in feeding strategy.

Although choristoderes were not closely related to crocodyliforms, they have often been described as eco-analogues of crocodilians due to general features of skull and body shape (e.g. Fox 1968; Erickson 1987; Evans & Hecht 1993). The slender-snouted *Champsosaurus* has been described as a gavial-like reptile, and it is interpreted as feeding on schools of fish, while the more robust *Simoedosaurus* has been compared with the broader-snouted crocodilians that take single prey items (Evans & Hecht 1993; Matsumoto & Evans 2010). The similar snout morphologies of *Gavialis gangeticus* and *Champsosaurus* evolved by convergence, and may reflect their specialised feeding behaviour. However, this similarity has also developed within, and been constrained by, a phylogenetic framework, and thus detailed differences between these taxa (e.g. cervical morphology, presence or absence of palatal dentition) may also be reflected in their feeding behaviour (Matsumoto & Evans 2016). Choristoderes and crocodilians may therefore provide a good example for the exploration of morphological convergent evolution. Furthermore, morphological variation within choristoderes, for example between *Champsosaurus* and *Simoedosaurus,* also provides important clues about ecological adaptation. Where these two genera coexist, such as in Paleocene localities of Europe and North America (e.g. Mont-Berru,

France; Fort Union Formation), they presumably divided the niche by feeding habit (Matsumoto & Evans 2010), as occurs in coexisting extant crocodilians with varied snout morphology (Brochu 2001).

Through evolutionary history, various aquatic reptile lineages independently developed a flattened skull with an elongated snout (platyrostry), including mesosaurids (parareptiles), pleurosaurs (rhynchocephalians), thalattosaurs (indet. diapsids), and crocodylomorphs (archosaurs). A similar adaptation was seen in some anamniotes (e.g. lonchorhynchine temnospondyls). This raises the question as to whether the dorsoventrally compressed skull morphology of neochoristoderes is an adaptation to reduce drag. If it was the case, then lateral head and neck movements may have been essential during feeding, and this functional adaptation should be reflected in their neck morphology. Although many studies have examined tooth and skull morphology to understand prey type and feeding behaviour (e.g. Busbey 1995; Evans & Sanson 1998; Gignac et al. 2019; Langston 1973; Massare 1987), less attention has been paid to neck mobility and range of flexion.

In order to investigate the feeding behaviour of choristoderes, this study focused on lateral snapping (lateral flexion) and tossing (dorsi-flexion) movements. Axial torsion and ventro-flexion are considered to be less involved in these feeding movements (as opposed to locomotion, e.g. Molnar et al. 2015), and will be analysed in a future study. To estimate the range of lateral and dorsi-flexion in the cervical column of extinct choristoderes, such as *Champsosaurus* and *Simoeodosaurus,* we first explored the functional morphology of cervical vertebrae contributing to lateral and dorsal neck movements in *Gavialis gangeticus* by comparison with short-snouted crocodilians. This resulted in the development and validation of a method to estimate the maximum angle of neck dorsi-flexion, which could then be applied to the extinct taxa.

INSTITUTIONAL ABBREVIATIONS

AMNH, American Museum Natural History, New York, USA; **CMN**, Canadian Museum of Nature, Ottawa, Canada; **IRSNB**, Institut Royal des Sciences Naturelles de Belgique, Brussels, Belgium; **KPM**, Kanagawa Prefectural Museum of Natural History, Odawara, Japan; **MNHN**, Muséum National d'Histoire Naturelle, Paris, France; **RTMP**, Royal Tyrrell Museum of Palaeontology, Drumheller, Canada; **SMM**, The Science Museum of Minnesota, St. Paul, Minnesota, USA; **UMUT**, The University Museum, The University of Tokyo, Tokyo, Japan; **UMZC**, University Museum of Zoology, Cambridge, UK.

MATERIALS

Post-atlantal cervical vertebrae (v2–9) of neochoristoderes were examined, and compared to those of extant crocodilians (Supp. Table S1). The morphology and articulation of the atlas (v1) is distinct from that of other cervical vertebrae. To simplify our estimates of the range of cervical flexion, the atlas was excluded from this analysis and will form the basis of a separate project.

Neochoristodera: Six specimens, each representing well-preserved serial cervical vertebrae, were selected from six well-established *Champsosaurus* species: the Late Cretaceous *C. albertensis*, *C. natator*, *C. ambulator*, and *C. laramiensis*, and the Palaeocene *C. gigas* and *C. dollo*. In addition, the study included fourteen Paleocene specimens of *Simoedosaurus*, representing *S. dakotensis* and *S. lemoinei*, although no specimen of *S. lemoinei* preserves a complete series of cervical vertebrae.

Extant Crocodylia: The species examined were taken from each crocodilian family (Alligatoridae, Crocodylidae, Gavialidae), and were selected based on snout morphology, mainly using the morphotype categories of Busbey (1995): long-snouted species, *Gavialis gangeticus* (*n*=6) and *Tomistoma schlegelii* (*n*=3); long and wide snouted species, *Crocodylus actus* (*n*=1); short/ medium-snouted species, *Alligator mississippiensis* (*n*=3), *Alligator sinensis* (*n*=1), *Caiman latirostris* (*n*=2),

Caiman crocodilus (*n*=2), *Osteolaemus tetraspis* (*n*=1), *Crocodylus niloticus* (*n*=1), and *Paleosuchus palpebrosus* (*n*=1). These specimens were mostly adult or semi-adult, based on size, but specimens of several ontogenetic stages were included for the reference taxa, *Gavialis gangeticus* and *Alligator mississippiensis*. Our preliminary study of the cervical vertebrae of *Gavialis gangeticus* revealed some ontogenetic variation. We therefore included different ontogenetic stages in the study to examine the effect of age class on intervertebral flexibility.

METHODS

The centrum length (CL), centrum height (CH), and neural spine height (NH) were measured for all cervicals (v2–9) in extant crocodiles and choristoderes (Fig. 2A, B). The distribution of aspect ratios of the centrum length/ height (CL/CH), and the neural spine and centrum heights (NH/CH) were summarised with a boxplot for *Champsosaurus*, *Simoedosaurus*, and extant crocodilians. These values have previously been used to characterise cervical morphology and also to compare cervical morphology within and between groups of both extant crocodilians (e.g. Iijima & Kubo 2019) and choristoderes (Matsumoto 2011).

In addition to these measurements, four morphological Indices, as listed below, were estimated for each cervical element in extant crocodilians and choristoderes (Fig. 3). These Indices were validated with data on the dorsal- and lateral-flexion capabilities of inter-cervical joints in extant crocodilians using CT images (Fig. 4). All measurements were recorded to the nearest 0.01 mm using digital calipers.

In all analyses, the cranio-caudal axis of the centrum was defined as the line connecting the ventral margins of the anterior and posterior articular facets of the centrum, because the midline cannot be identified from lateral views of centra (Fig. 2A, B). This ventral line is almost parallel to the floor of the neural canal (Fig. 2C). The intervertebral joints, e.g. v2 and v3, are described as v2/v3 and the vertebral range is indicated by an em-dash, e.g. v2–4.

Index 1: Enclosed Zygapophyseal angles (EZA) as a measure of dorsal and lateral range of flexion (Fig. 3A, B): Cervical vertebrae were photographed in both anterior and posterior views, and the EZA (=enclosed zygapophyseal angle, see Fig. 3A, B) of pre- (α_{ant}°) and post- (α_{post}°) zygapophyses respectively were measured on each digital-photograph to the nearest 1°, as applied in several previous studies (e.g. Hua 2003; Molnar et al. 2014, 2015; Pierce et al. 2011). This value (EZA) was used, instead of the angle of the zygapophyses in relation to the horizontal, because the latter can be difficult to judge or to measure accurately. In this context, a high EZA (α = ~180°) implies that zygapophyses are horizontal in anterior/ posterior view, whereas a low EZA (α = < 90°) indicates that they are more vertical in anterior/posterior views. The EZA is considered to reflect dorso-ventral and bilateral flexibility at the intervertebral joints (Hua 2003). A relatively low EZA (zygapophyseal surfaces almost vertical) would facilitate dorso-ventral intervertebral motion, whereas a relatively large EZA (zygapophyses almost horizontal) would facilitate bilateral motion (Hua 2003; Pierce et al. 2011; Molnar et al. 2014, 2015). In some cases, zygapophyses are incomplete/ distorted in fossil taxa. Measurements were not taken when cervical vertebrae had been distorted on both sides of the zygapophysial plate (left/ right). However, when one side of the zygapophyseal plate was less distorted (or complete), the EZA was measured from the reconstructed image by mirroring about the sagittal axis.

Index 2: Moment arm of dorsi-flexor muscles in relation to the neck length (Fig. 3C–D): In crocodilians, the skull and the neck are dorsiflexed by bilateral contraction of the m. transversospinalis cervicis and m. longissimus cervicis (Cleuren & De Vree 2000). These two muscles run above the centrum nearly parallel to the craniocaudal axis. Of these muscles, the m. transversospinalis cervicis, which connects the cervical neural spines, provides the largest dorsi-flexion moment arm. The distance from the pivot of the inter-central joint to the distal end of the neural spine can be regarded as an Index for the muscle moment arm. A relatively large moment

arm at each inter-cervical joint in relation to the total neck length indicates an ability for more powerful dorsi-flexion, or a greater stability against ventro-flexion (e.g. Iijima & Kubo 2019).

In an intervertebral joint, the position of the pivot of dorso-ventral rotation depends on the shape of the inter-central joint. In procoelous joints (e.g. crocodilian cervicals), the pivot point is at the centre of curvature of the posterior condyle or anterior cotyle, respectively (e.g. Fronimos & Wilson 2017). Therefore, the moment arm of the dorsi-flexor muscle for each cervical joint was estimated by taking the distance from the pivot point of the inter-central joint to the distal-most point of the neural spine using centrum height (CH) and neural spine height (NH) in the following equation: (0.5 × CH) + NH [mm] (Fig. 3C).

However, according to studies of the amphiplatyan joint in mammals, the pivot point is not stable, but shifts between the centre of the inter-central joint and its dorsal-most point (Shapiro 1995; Long et al. 1997; Kowalski et al. 2005). Therefore, we can assume that the pivot point lies between the centre and the dorsal-most point of the amphiplatyan inter-central joint in extinct taxa as well (e.g. choristoderes). Here, we estimated the possible maximum (M_1) and minimum (M_2) moment arms in *Champsosaurus* and *Simoedosaurus*. The maximum moment arm is calculated as the distance from the centre of the inter-central joint to the tip of the neural spine (M_1= (0.5 × CH) + NH [mm]: Fig. 3C), whereas the minimum moment arm is regarded as the distance from the dorsal-most point of the joint to the tip of the neural spine (M_2= NH [mm]: Fig. 3D).

The moment arm of the dorsi-flexor muscles in relation to the total neck length was estimated in those crocodilian and choristodere study specimens for which cervicals v2–9 were available. The total neck length was estimated as the sum of the centrum lengths (CL) of the eight successive cervical vertebrae from v2 to v9. In the case of the *Simoedosaurus dakotensis* specimen (SMM 76.10.1) in which v9 was not preserved, the total neck length was estimated as eight times the average CL of the seven available cervicals (v2–8). The tip of the neural spine lies roughly above the caudal articular surface of the centrum in the study species. Therefore, for the inter-central joint between any two successive cervicals, the distance between the pivot point and the tip of the neural

spine of the anterior member likely reflects the moment arm of the joint. The dorsi-flexor moment arm varies according to the inter-cervical joint position within the specimen. The relationship between the relative position of the inter-cervical joint (v2/v3–v8/v9) [horizontal axis] and the dorsi-flexor moment arm [vertical axis], which were both normalized by the total neck length, was plotted for each specimen and compared between taxa.

Index 3: Orientation of the pre-zygapophysis and its facet in relation to the pivot point of the inter-central joint (Fig. 3E–F): To assess the potential range of dorsi-flexion, pairs of consecutive cervical vertebrae were re-articulated. Although this can easily be done in extant species with complete cervical vertebrae, in fossil taxa vertebrae may be too fragile to re-articulate. Here we propose a new Index for fossil taxa, which requires only one side of a cervical vertebra (i.e., the vertebra does not need to be complete or undistorted on both sides).

In dorsi-flexion between two successive cervicals, the anterior cervical can be thought of as rotating about the pivot of the inter-central joint, and the post-zygapophysis of the anterior cervical slides over the pre-zygapophysis of the more posterior cervical (Fig. 3E). Dorsi-flexion about the pivot stops when the pre-zygapophysial facet of the more posterior cervical fully occupies the concavity anterior to the post-zygapophysial facet of the anterior cervical (Kusentsov & Tereschenko 2010). The degree of dorsi-flexion permitted can therefore be expressed by comparing two angles. The first is that between the line through the pivot parallel to the cranio-caudal long axis and a line through the pivot to the anterior margin of the post- zygapophysial facet of the anterior cervical (Fig. 3E: β_{post}°). The second is the angle between a line through the pivot parallel to the cranio-caudal long axis, and a line through the pivot and the tip of the pre-zygapophysis of the posterior cervical (Fig. 3E: β_{ant}°). The difference between angle β_{post} and angle β_{ant} should reflect the degree to which the anterior cervical can dorsi-flex in relation to the posterior cervical: the greater the difference between angle β_{post}° and β_{ant}° (β_{ant}°-β_{post}°) the greater the potential for dorsi-flexion.

As described above, the pivot position depends on the joint morphology. In crocodilians, the pivot point is estimated to lie at the centre of curvature of the posterior condyle or anterior cotyle, and the angle "β_{ant}°-β_{post}°" is measured on this basis (Fig. 3E). On the other hand, in choristoderes, the pivot point is estimated to lie between the centre of the concave inter-central joint and its dorsal-most point. Therefore, the angle "β_{ant}°-β_{post}°" was measured for two different pivot positions—the centre of the inter-cervical joint and its dorsal-most point, respectively—assuming that the angle fits within this range (Fig. 3F). These angles were measured on digital photographs of consecutive pairs of cervical vertebrae taken in lateral view.

Index 4: Maximum inter-cervical angle of dorsi-flexion in articulation (Fig. 3G): As an alternative to Index 3, the maximum inter-cervical angle of dorsi-flexion estimated by the re-articulation of consecutive pairs of cervicals was calculated for extant crocodilians (Fig. 3G). To do this, pairs of consecutive cervicals were articulated into the most dorsi-flexed position possible and then photographed in lateral view. With the cranio-caudal long axis of the centrum defined as in Index 3, we measured the angle between the cranio-caudal axis of the dorsi-flexed anterior member of the vertebral pair in relation to the cranio-caudal axis of the posterior member (Fig. 3G: γ°). This angle represents the maximum angle of dorsi-flexion at that intervertebral joint. The measurement was repeated between consecutive pairs of vertebrae along the cervical vertebral column. Indices 3 and 4 were both calculated for extant crocodilians, but Index 4 could not be applied to fossil taxa due to the risk of damage to fragile specimens. The reliability of these two Indices was evaluated and compared in extant crocodilians using μCT (see Validation) before they were applied to choristoderes.

Validation: Inter-cervical angles of dorsi-flexion and bilateral flexion measured *in situ* on fresh specimens (Fig. 4A–C): To test whether Indices 1–4 provide an accurate estimate of joint

flexibility in extant species, we used micro-computed tomography (μCT) to examine and quantify inter-cervical flexibility. Fresh specimens of semi-adult *Gavialis gangeticus* (KPM-NFR 52) and *Caiman latirostris* (KPM-NFR 54) were μCT scanned in several cervical postures. The cervical postures used were defined by the orientation of the skull and neck in relation to the trunk as follows: Standard, the skull in neutral position with its rostrum directed anteriorly and the dorsum facing upward, and the neck in a resting position (Fig. 4A); Upward, the skull and neck in the most dorsi-flexed position possible without dislocating any joints (Fig. 4B); Lateral-flexed, the skull with the dorsum facing upward and the neck flexed in the horizontal plane into the most lateral position possible without dislocating any joints (Fig. 4C). The skull was moved into each of these extreme positions, fixed on a board with tape and styrofoam blocks, and a CT scan was performed. At this time, it was assumed that the cervical vertebrae and the skull were interlocked. However, the maximum Upward and Lateral-flexed postures were defined from the overall position of the skull in relation to the trunk. It is therefore not possible to confirm that every intercervical joint had reached its maximum dorsi- or lateral flexion angle, and in some parts of the neck dorsi-flexion may be limited by the placement of overlying osteoderms (see below). Torsion of the skull about the cranio-caudal axis was not examined.

The specimens were scanned at the National Museum of Nature and Science, Tokyo, Japan, using a TESCO, Microfocus CT TXS 320-ACTIS (slice width 0.1 mm). The scanned images were imported into the three-dimensional visualization software Avizo 8.0 (FEI Visualization Science Group, Burlington, USA), and the skull and each element of the cervical series were segmented out. A line along the ventral margin of the centrum in lateral view was used to orientate each vertebra.

For each neck posture (Standard, Upward, and Lateral-flexed), the dorso-ventral and bilateral inter-cervical joint angles were measured for seven joints between v2–9 in both *Gavialis gangeticus* and *Caiman latirostris* (Fig. 4). On the basis that the line connecting the ventral margins of the centrum is nearly parallel to the neural canal (Fig. 2C, cross-section), the unit-vector of the line was defined as the orientation of the cranio-caudal axis of each cervical. The dorsal-ward and lateral-

ward unit-vectors perpendicular to the cranio-caudal axis were defined as the orientations of the dorso-ventral and medio-lateral axes of each cervical vertebra (Supp. Fig. S1). The three unit-vectors were determined for each isolated cervical element (Supp. Fig. S1b), and then the cervicals associated with the unit-vectors were each superimposed on the corresponding cervical element *in situ* for the three different neck postures (Standard, Upward, and Lateral-flexion) (Supp. Fig. S1c).

Within a consecutive pair of cervical vertebrae, the orientation of the anterior member in relation to the posterior member *in situ* was described by Euler angles, which were estimated using the difference between each of the unit-vector orientations of the two cervicals in the pair. The anterior vertebra was rotated around its dorso-ventral (yaw: right lateral flexion as positive), medio-lateral (pitch: dorsi-flexion as positive), and cranio-caudal (roll: right-ward torsion as positive) axes in sequence. The angles of dorsi-flexion ($\theta°$), lateral flexion ($\phi°$), and torsion were estimated for the joints (v2/v3–v8/v9).

The angle between the cranio-caudal axes of the anterior and posterior members of each successive cervical pair (Supp. Fig. S2: $\theta°$) was measured for the Standard ($\theta_{st}°$), Upward ($\theta_{up}°$), and Lateral ($\theta_{lat}°$) postures. The difference between the Standard ($\theta_{st}°$) and Upward ($\theta_{up}°$) angles indicates actual dorsal mobility of the joint ($\theta_{up}°$-$\theta_{st}°$). This value was compared with that estimated from Indices 1–4. Likewise, the range of lateral flexion angles at the inter-cervical joint was measured for the Standard ($\phi_{st}°$), Upward ($\phi_{up}°$), and Lateral ($\phi_{lat}°$) postures (Supp. Table S2). The angle of inter-cervical lateral flexion ($\phi_{lat}°$) obtained by this method was compared with that obtained from Index 1.

DESCRIPTION OF CERVICAL VERTEBRAL MORPHOLOGY

Choristodera (Supp. Fig. S3, 4)

The cervical region of *Champsosaurus gigas* (**Supp. Fig. S3**) and *Simoedosaurus dakotensis* (**Supp. Fig. S4**) was described by Erickson (1987), and can be characterised as follows: cervical count nine; axis inter-centrum attaching to the ventral portion of the atlas pleurocentrum;

cylindrical and amphiplatyan centra; closed notochordal canal without central pit; neurocentral sutures remaining open in the adult; parapophysis and diapophysis separated in anterior cervical vertebrae, not completely merged until v9; posteriorly bifurcated spine table of axis, arrow-shaped in dorsal view with rugose ornamentation; neural spines rectangular in lateral view; neural spines gradually increasing in height from v3 to v5, and the spines of the remaining cervicals almost equal in height to those of trunk vertebrae; neural spines with strongly developed rugosity and/or ridges on anterodorsal margins.

Comparison between species (e.g. *S. lemonei, C. natator*, *C. dolloi*, *C. albertensis*) provides further detailed information on the neural spine, centrum and zygapophyseal morphology. The neural spine is posteriorly inclined in most *Champsosaurus* species (e.g. *C. gigas* and *C. amburator*) but is almost vertical in *Simoedosaurus*. The neural spine tables are transversely narrow (except v2) in *Champsosaurus* (**Supp. Fig. S3**), but *Simoedosaurus* cervicals v2–5 (v6 in *S. limoinei*) have a relatively blunt, bifurcated spine table with rugose ornamentation (**Supp. Fig. S4**). Furthermore, *Champsosaurus* is unique in having horizontal zygapophyseal facets in the cervicals posterior to v7. In some *Champsosaurus* species, the bilateral zygapophyses are merged at the midline to form a single median facet (e.g. *C. dolloi*; IRSNB 1582). *Champsosaurus* cervical centra bear midventral keels throughout the neck (v2–9) (**Supp. Fig. S3**). By contrast, midventral keels are limited to the anterior portion of the neck in *Simoedosaurus* (v2 in *S. dakotensis*, v2–4 in *S. limoinei*), with posterior centra bearing a strongly developed rugosity on the ventral surface of the centrum. The presence of an accessory spinous process below the post-zygapophysis is characteristic of *S. dakotensis* (v6–8), but *S. lemoinei* has only weakly developed tubercles in this position (v5–9; pers. obs RM). *Simoedosaurus* also shows strong traces of attachment sites for both epaxial and hypaxial muscle groups on the dorsal and lateral surfaces of the neural spines and on the ventral surface of the centra respectively.

Crocodylia (Supp. Fig. S5, 6)

The neck of extant crocodilians has the following general features: cervical vertebral count nine; procoelous centra (ball and socket joint); atlas consists of the paired neural arches and intercentrum; V-shaped pro-atlas overlapping the atlas neural arch; odontoid process (atlas pleurocentrum) fuses with the axis during ontogeny; cervical neural spines roughly rectangular in lateral view (cranio-caudally wider than high); centra bear hypapophyseal keel, appearing anteriorly on either v2 or v3, and gradually increasing in depth posteriorly; tip of hypapophyseal keel directed anteriorly; pre- and post-zygapophyses oval and with a flat articular surface; articular surfaces of the centrum either circular or square; parapophysis and diapophysis separate; and diapophysis becoming laterally expanded and more dorsally positioned in posterior cervicals. However, some morphological variation is evident within crocodilians in centrum shape and in neural spine height and angle (Hoffstetter & Gasc 1969). *Gavialis gangeticus* is characterised by having cranio-caudally elongate centra with relatively short neural spines (Supp. Fig. S5), in contrast to more typical crocodilians like *Alligator mississippiensis* in which the cervical centra are cranio-caudally short with tall neural spines (Supp. Fig. S6). Although the neural spines are rectangular in lateral view in most crocodilians (including the long-snouted *Tomistoma schlegelii* and *Crocodylus acutus*), *Gavialis gangeticus* has triangular spines on v3–5 in juveniles, and slender trapezoid spines with a dorsally pointed tip on v3–5 in adults. In most crocodilian species, the middle part of the neck (v5–7) bears cranio-caudally narrow neural spines in lateral view while anterior and posterior cervical spines are relatively wide. Moreover, neural spines are usually either vertical or posteriorly inclined (prominently inclined in *Tomistoma schlegelii* and *Crocodylus acutus*), but in some small crocodilians (e.g. *Osteolaemus tetraspis* and *Alligator sinensis*) the spines in the middle portion of the neck are anteriorly inclined. These angles and the antero-posterior widths of the neural spines in lateral view may be related to the degree of flexibility of the neck in different planes.

RESULTS FOR CROCODYLIA 1) Centrum and neural spine profile in Crocodylia (Fig. 5)

As outlined above, the cervical vertebrae of *Gavialis gangeticus* are distinguished from those of other crocodilians in having cranio-caudally elongated centra (range of CL/CH: 1.3–1.6) and low neural spines (range of NH/CH: 1.1–2.5). In *G. gangeticus*, the largest individual (G5 in Fig 10: KPM-NFR 92) shows slightly greater values for CL/CH and NH/CH than the smallest specimen (G3 in Fig 5). By contrast, short/ medium-snouted crocodilian species (e.g. *Alligator mississippiensis*, *A. sinensis*, *Caiman crocodilus*) resemble one another in having relatively short centra (CL/CH: 0.5–1.0) and tall neural spines (NH/CH: 1.4–3.5). Cervical morphology in the long-snouted *Tomistoma schlegelii* varies through ontogeny—small specimens (UMUT 12279) closely resemble *G. gangeticus* (Fig. 5) but the vertebrae of more mature specimens were intermediate between those of *G. gangeticus* (long centra, low spines) and *Alligator mississippiensis* (short centra, tall spines) (CL/CH: 1.3–2; NH/CH: 1.5–2.9). Although *Crocodylus acutus* was categorised as long-snouted by Busbey (1995), the snout is slightly wider than in *G. gangeticus* and its cervical vertebrae are more similar to those of the short/ medium-snouted crocodilians.

2) Index 1: Enclosed Zygapophyseal Angle (EZA: Fig. 6)

In *Gavialis gangeticus*, the Enclosed zygapophyseal angles (EZA: α_{ant} and α_{post}) were mostly less than 90°, except at the inter-cervical joint between v2 and v3 (α = ~130°). In a large specimen of *G. gangeticus* (snout-tail length [STL] ~3 m; KPM-NFR 92), the EZAs of the posterior inter-cervical joints (v7/v8–v8/v9) were slightly greater (α = 91–98°) than those of the smaller individuals (STL ~1 m in KPM-NFR 18, 52; α = 55°–66°). Although there is some ontogenetic variation, the general trend of EZAs was similar among all specimens of *G. gangeticus* examined. A low EZA facilitates dorso-ventral motion (steeply angled zygapophyses) and a high EZA (horizontal zygapophyses) facilitates bilateral motion (Hua 2003; Pierce et al. 2011; Molnar et al. 2014, 2015). Although the EZAs do not strictly control the dominant vertebral motion, as EZAs gradually change along the vertebral column, they are considered to be a reasonable guide to the direction of optimum mobility. The EZAs of *G. gangeticus* suggest that bilateral motion is the main movement in the most anterior

414 portion of the neck, whereas the remaining cervicals are adapted for dorso-ventral flexion.
415 *Tomistoma schlegelii* also has steeply angled zygapophyses (EZA, α = ~70°–100°), but this
416 includes the anterior portion of the neck, unlike *G. gangeticus*.
417 Short/medium snouted crocodilian species generally have high values of EZA (α = ~100°–
418 130°) all along the cervical vertebral column (e.g. *Alligator mississippiensis*, *Caiman latirostris*,
419 *Alligator sinensis*, *Paleosuchus palpebrosus*) (Fig. 6, Supp. Fig. S7). However, there is some
420 variation among species. For example, *Crocodylus niloticus* has nearly horizontal zygapophyses (α
421 = ~190°) in the anterior part of the neck (v2/v3 joint: Supp. S2B), whereas EZA is somewhat lower
422 in the anterior neck (v2/v3 joint: α = 90°–130°) of most other species (Fig. 6, Supp. Fig. S7). In
423 addition, *Osteolaemus tetraspis and Crocodylus acutus* are unique in having steeply angled
424 zygapophyses (α < 90°) along the whole neck (Supp. Fig S7). Ontogenetic variation was recorded
425 in the anterior to middle part of the neck (v3/v4–v4/v5) in *Alligator mississippiensis* where the
426 zygapophyses were found to have low values of EZA (α = ~90°) in a young individual (STL, ~1.2 m;
427 KPM-NFR 16), but higher values (α = ~120°) in a larger adult (STL, ~3 m; KPM-NFR 109) (Fig. 6C).
428 Taken together, these results suggest that the neck in most short/medium-snouted crocodilian
429 species is adapted primarily for bilateral flexion.
430
431 **3) Index 2: Moment arms of dorsi-flexor muscles (Fig. 7A)**
432 Towards the posterior part of the cervical region, the moment arm of dorsi-flexors relative to the
433 length of the whole neck (v2–9) (i.e. M_1 dorsi-flexor moment arm/ total neck length) increases.
434 Among the crocodilians examined, *Alligator mississippiensis* and *Osteolaemus tetraspis* appear to
435 have the largest values of moment arm relative to neck length (v2/v3, ~0.20; v8/9, ~0.35), followed
436 by *Caiman* and then the other species. In contrast, *Gavialis gangeticus* had the smallest values of
437 moment arm relative to neck length, which are roughly half those of *O. tetraspis* (v2/v3, ~0.13;
438 v8/v9, ~0.22). This applies particularly to the larger individuals of *G. gangeticus* (KPM-NFR 92). In
439 *Tomistoma schlegelii*, the relative moment arms were slightly larger than those of *G. gangeticus*,

with values intermediate between those of *G. gangeticus* and other crocodilians (v2/v3, 0.16; v8/v9, ~0.23). Thus, the mechanical efficiency of dorsi-flexor muscles relative to the neck length seems to be relatively poorer in *G. gangeticus* than in other crocodiles.

4) Index 3: Estimated maximum angle of inter-cervical dorsi-flexion (Fig. 8)

As described above (Methods), Index 3 compares two angles in successive pairs of cervical vertebrae. The first angle, on the anterior member of each pair, is that between the cranio-caudal axis and a line connecting the pivot point of the centrum to the concavity anterior to the post-zygapophysial facet (Fig. 3E: β_{post}°). The second, on the posterior member of each pair, is the angle between the cranio-caudal axis and a line connecting the pivot point of the centrum and the tip of the pre-zygapophysis (Fig. 3E: β_{ant}°). The difference between these angles is summarised in Figure 8 (A, B) where the value β_{post}°-β_{ant}° is plotted on the Y axis. The estimated maximum angle of dorsi-flexion varies through the cervical series among crocodilian groups, but each inter-cervical joint generally flexes no more than 30° (Fig. 8A, B). Our results for *Alligator mississippiensis* are comparable with those of Fronimos & Wilson (2017), and both the maximum angle of dorsi-flexion (error ~5°) and its peak point were the same in each study. The negative angles indicate an inability to dorsi-flex. The inter-cervical joint of v2/v3 generally shows the least flexibility in all crocodilians, particularly in *Gavialis gangeticus* and *Caiman latirostris* (< 5°), (Fig. 8; Supp Fig. S8). Further posteriorly (v3–9), *G. gangeticus* shows a fairly consistent capacity for dorsi-flexion at roughly ~10°–15° for each joint through the cervical series. *Tomistoma schlegelii* (Supp. Fig. S8) is broadly similar to *G. gangeticus* in the degree of cervical dorsi-flexion. In *G. gangeticus*, the angle of dorsi-flexion was examined in specimens representing several different ontogenetic stages from young to adult (KPM-NFR 18, 52, 92). Although the young individual had only weakly ossified condyles, the degree of dorsi-flexion was roughly similar between all specimens of this species (Fig. 8; Supp. Fig. S8).

5) Index 4: Maximum inter-cervical angle of dorsi-flexion estimated by re-articulation (Fig. 8A, B)

The maximum degree of dorsi-flexion permitted at each inter-cervical joint was estimated by re-articulating consecutive pairs of cervical vertebrae (Fig 3G: γ°), and is also shown in Figure 8A, B and Supp. Figure S7, as well as being compared with the results derived from Index 3 (Fig. 3E: $\beta_{post}{}^{\circ}$-$\beta_{ant}{}^{\circ}$). The differences between the angles estimated by Indices 3 and 4 were generally less than 10° in all crocodilians examined (Fig. 8A, B; Supp. Fig. S8). The plot lines of Index 3 essentially overlap those of Index 4 (Fig. 8A, B: Supp. Fig. S8).

6) Validation of Indices

To test whether Indices 1–4 provide an accurate estimate of actual cervical dorsi-flexion in extant (and then extinct) species, µCT examination was conducted to quantify inter-cervical flexibility in fresh specimens. The absolute values for torsion about the cranio-caudal axis of the seven inter-cervical joints (v2/v3–v8/v9) for the three different neck postures were shown to be negligible in both *Gavialis* (0.66º–2.22º in the interquartile range) and *Caiman* (0.85º–1.86º in the interquartile range) (Supp. Table S2). The dorsi- (θ) and lateral (ϕ) flexion angles obtained are described below.

Inter-cervical articulation angles in the Standard posture (Fig. 8A, B; 9A, E): The µCT scan taken with specimens in Standard (=neutral) posture (Fig. 4A), show that the neck of *Gavialis gangeticus* at rest has a gentle curvature throughout the cervical series with the middle part of the neck (v5–7) at the bottom of the curve (Fig. 9A). The inter-cervical joints are slightly dorsi-flexed ($\theta_{st}{}^{\circ}$, ~5°) in the middle to posterior neck (v5/v6–v8/v9), whereas the anterior part of the neck (v2/v3, v3/v4) is ventro-flexed ($\theta_{st}{}^{\circ}$, ~–10°, Fig. 8A).

The neck of *Caiman laterostris*, in contrast, shows a deeper curvature in the Standard posture (Fig. 9E), with the inter-cervical joints in the posterior part of the neck (v6/v7–v8/v9)

showing a relatively large angle of dorsi-flexion (θ_{st}°, ~10°), and those in the anterior to middle region (v2/v3–v5/v6) showing a smaller angle (θ_{st}°, >5°: Fig. 8B).

Cervical vertebral proportions, and the height of the neural spine, as well as skull height may affect the overall depth of the cervical series and therefore the degree of neck curvature in the Standard posture. However, additional studies are required to test this hypothesis.

Inter-cervical angles of dorsi-flexion in the Upward posture compared with Indices 1–4: The µCT images of *Gavialis gangeticus* demonstrated that the maximum angle of inter-cervical dorsi-flexion (θ_{up}°) at the v3/v4 joint was ~20°, with joints in the anterior part of the neck (v2/3–v4/v5) contributing most of the movement (θ_{up}°-θ_{st}°, ~10° at each inter-cervical joint). These results for the anterior part of the neck (v2/3–v4/v5) are consistent with those obtained using Indices 3 and 4 (β_{post}°-β_{ant}° and γ°: Fig. 8A, Supp. Table S2). However, more posterior inter-cervical joints (v5/v6–v8/v9: θ_{up}°) were only slightly flexed (up to ~5°), and there was no difference in inter-cervical joint angle between the Standard and Upward postures (θ_{up}°-θ_{st}°) (Fig. 8A, Supp. Table S2). Nonetheless, these posterior joints have the potential for additional dorsi-flexion, as indicated by Indices 3 and 4 (β_{post}°-β_{ant}° and γ°, ~15°). Both the maximum angle of dorsi-flexion (θ_{up}°) and the potential mobility of dorsi-flexion beyond the neutral position (θ_{up}°-θ_{st}°), were consistent with the estimated dorso-ventral flexibility indicated by Index 1 (EZAs, α < 90°: Fig. 6A).

The size and the distance between the osteoderms (Fig. 9B) may also influence the potential for dorsi-flexion (θ_{up}°-θ_{st}°). Although there is potential for dorsi-flexion in posterior cervical vertebrae as well as in the middle-portion of the neck, dorsi-flexion occurs preferentially at v3/v4 and v4/v5 in *G. gangeticus*. The overlying osteoderms are small and well-separated in the anterior cervical region, where the joints are flexible, whereas they are large and close together in the mid-posterior portions of the neck, where the joints are less flexible. The elements of the anterior-most osteoderm pair are small and circular, lying above v1/v2 (Fig. 9B). There are no osteoderms above the joint

between v2 and v3, whereas relatively large squared osteoderms start from the level of v4. The osteoderms associated with v4 cover only that vertebra, and there is a relatively wide space between them and the anterior osteoderms above v1/v2. As this region of the neck shows the maximum permitted angle of dorsi-flexion, it would seem that the arrangement of osteoderms does not restrict neck movement. However, the pair of osteoderms lying above v5/v6 is the largest in cervical region, and may limit dorsi-flexion. Further posteriorly, the osteoderms gradually become smaller, and overlying v7–v9 they are placed on each vertebra. There are spaces between these osteoderms, but the spaces reduce further posteriorly and may limit flexibility.

Angles measured from the µCT data of *Caiman latirostris* demonstrated that the middle-posterior part of the neck (v4/v5–v7/v8) makes a major contribution to overall dorsi-flexion (θ_{up}°, ~10° –25° at each inter-cervical joint), especially at the v6/v7 joint (θ_{up}°, ~25°) (Fig. 8B, Supp. Table S2). The estimates provided by Indices 3 (β_{post}°-β_{ant}°) and 4 (γ°) were generally consistent with the maximum degree of dorsi-flexion recorded by µCT (θ_{up}°), with errors of <~ 10° (Fig. 8B, Supp. Table S2). The µCT θ_{up}° angle matched that estimated by Index 3 (β_{post}°-β_{ant}°) very well in most of the neck, but the match was poorer at the anterior inter-cervical joints (v3/v4). Possible causes of mismatch for the Upward posture may be the distribution of dorsal osteoderms (Fig. 9F). In the µCT-scans of the Upward posture, the osteoderms were seen to be closely packed in the middle and posterior cervical area, whereas there was some space between the osteoderms in the anterior neck (as noted above). Therefore, as proposed above, the anterior inter-cervical joints observed in the µCT-scans (θ_{up}°) may have additional potential for dorsi-flexion. Comparison of the plots of inter-cervical angle in the Standard neck posture (θ_{st}°) and the Upward posture (θ_{up}°), shows close similarity between the two neck positions (Fig. 8B, Supp. Table S2). In the middle-posterior neck joints (~v5/v6–v8/v9), the potential degree of dorsi-flexion from the Standard posture (θ_{up}°-θ_{st}°) was more than 10°, whereas in the anterior neck (v2/v3, v3/v4) the value (θ_{up}°-θ_{st}°) indicated that dorsi-flexion was limited to ~5° (Fig. 8B, Supp. Table S2). *Caiman latirostris* yielded similar values of

EZAs throughout the neck (Index 1, ~100°: Fig. 6D), consistent with the findings outlined above that all inter-cervical joints have at least a moderate capacity for dorsi-flexion compared to those of the other crocodilians, such as *Gavialis gangeticus* and *Tomistoma schlegelii*.

The µCT scans of *Gavialis gangeticus* and *Caiman latirostris* showed that Index 1 (EZA) roughly reflects the potential for inter-cervical dorsi-flexion, but it is not accurate enough to estimate the actual angles of dorsi-flexion ($\theta°$). In addition, Index 2 (M) did not directly reflect the dorso-ventral flexibility of the joints. On the other hand, Indices 3 ($\beta_{post}°$-$\beta_{ant}°$) and 4 ($\gamma°$) are reliable predictors of maximum inter-cervical dorsi-flexion.

Thus Indices 3–4 can confidently be used to estimate cervical dorsi-flexion (Index 3) and the maximum angle of dorsi-flexion (Indices 3 and 4) in fossil taxa such as choristoderes. Index 3 is more applicable to fossil vertebrae that are relatively incomplete or too fragile to re-articulate (as required by Index 4). However, it is important to remember that the maximum angle of dorsi-flexion ($\theta_{up}°$) may also be limited by the distribution and size of the osteoderms (n/a in choristoderes), toughness of the skin, and the distribution and strength of muscles, tendons, and ligaments as tested by Molnar et al. (2015). However, Indices 1–4 may not accurately reflect angles of inter-cervical dorsi-flexion in a Standard (neutral) neck posture ($\theta_{st}°$), as the cervical column may not be horizontal, but curved, as observed in *Gavialis gangeticus* (Fig. 9A) and *Caiman latirostris* (Fig. 9E).

Angles of inter-cervical lateral flexion measured *in situ* compared with estimates from Index 1: In the µCT image of the lateral-flexed posture in *Gavialis gangeticus,* the angle of lateral flexion ($\phi_{lat}°$) varied along the neck (Fig. 8C, Supp. Table S2). The maximum lateral flexion mainly occurred in the anterior part of the neck (v2/v3: $\phi_{lat}°$, ~18°; v3/v4: $\phi_{lat}°$, ~21°; Fig. 8C, Supp. Table S2). The v2/v3 joint also has the highest value of EZA (α >90°) within the cervical series of this species (Fig. 6A). However, the v3/v4 joint has value of EZA (α <90°), although the joint showed the largest angle of lateral flexion in the µCT image. Lateral flexion was more limited ($\phi_{lat}°$ <~10°) in succeeding

joints (v4/v5–v7/v8), especially in the middle part of the neck (v5/v6–v6/v7: ~0°), corresponding to EZAs of <90° in these cervicals (Fig. 6A).

The potential degree of lateral-flexion, given by the maximum absolute lateral- flexion angles (ϕ_{st}°, ϕ_{up}° and ϕ_{lat}°), was increased in the v2/v3 (~18°) and v3/v4 (~21°) joints, whereas the angle was smallest (<10°) in the middle to posterior inter-cervical joints (v5/v6–v8/v9: Fig. 8C, Supp. Table S2). Although the specimen was CT-scanned in the Lateral flexed posture (Fig. 4C), the v4/v5–v5/v6 joints were more dorsally-flexed (θ_{lat}°, ~15°) than laterally flexed ($|\phi_{lat}|$, <5°) (Fig, 8A, Supp. Table S2). Thus, in *Gavialis gangeticus*, the v2/v3–v3/v4 inter-cervical joints have a greater potential for lateral-flexion, whereas the v4/v5–v5/v6 joints were further dorsally flexed, and the more posterior inter-cervical joints did not flex further laterally from their Standard postural positions (Fig. 8C).

In *Caiman latirostris*, lateral flexion at the inter-cervical joints is greater than 10°, except at the v2/v3 and v8/v9 joints (~8°), with maximum flexion achieved in the middle part of the neck (v5/v6: ~20°; Fig. 8D, Supp. Table S2). In this species, EZA is high (α, ~100°) throughout the neck, and the µCT data demonstrated that most inter-cervical joints (mainly v3/v4–v7/v8) contributed to lateral flexion as well as in dorsi-flexion as mentioned above. Overall, these results suggest that a high EZA (α, ~100°) may identify the main region of lateral flexion within the cervical series and allow for lateral-flexion of the neck in crocodilians.

RESULTS FOR CHORISTODERA

1) Centrum length and neural spine height (Fig. 5)

There are no significant differences between *Champsosaurus* and *Simoedosaurus* in centrum shape or neural spine height. In both fossil genera, the square centra are broadly similar to those of short-snouted crocodilians, whereas the short neural spines are more similar to those of *Gavialis*.

2) Index 1: Enclosed Zygapophyseal angles (EZA) (Fig. 10)

All species of *Champsosaurus* examined showed a general trend where by EZAs were high (α = ~100°–160°) in the anterior half of the neck (v2–4), and increased further in the middle to posterior cervicals (α = ~180°–220°), with the zygapophyseal articular surfaces becoming horizontal or even obtuse. In *Simoedosaurus dakotensis* (North America) EZA is relatively constant (α = 100°–125°) throughout the neck (v2–9), but in the European *S. lemoinei*, EZA is low (α = ~75°–95°) in the anterior to middle part of the neck (v2–5), and higher posteriorly (v6–9). However, no specimen of *S. lemoinei* preserves a complete cervical series and the results presented here are based on individuals representing various ontogenetic stages. Thus, the difference in EZAs between *Simoedosaurus* species might be due to ontogenetic variation, as recognised in crocodilians (e.g. *Gavialis gangeticus*, *Alligator mississippiensis*).

3) Index 2: Moment arm (M) of dorsi-flexor muscles in Choristodera (Fig. 7B)

In Choristodera, the pivot point of the centrum is taken to be either the centre or dorsal-most point of the amphiplatyan inter-central joint. Therefore, two arrangements of the pivot point were set up and the transition of the moment arms of the dorsi-flexors along the whole neck was compared (Fig. 7B). Regardless of the two arrangements of the pivot points, the moment arm transition patterns along the neck are generally similar in both *Champsosaurus* and *Simoedosaurus* (Fig. 7B) with their moment arms becoming greater (M= 0.2–0.3) in the middle portion of the neck (v6–8). When the pivot point is located at the centre of the joint surface, the values for the moment arms in relation to the neck length are between 0.17 and 0.29 in both genera, similar to that of *Caiman latirostris* (Fig. 7A). On the other hand, when the pivot is placed at the dorsal-most point of the centrum, the values are between 0.10 and 0.23 in choristoderes, a range that is similar to that of *Tomistoma schlegelii* and larger than that of *Gavialis gangeticus* in the middle portion of the neck (v4–8).

4) Index 3: Capacity for cervical dorsi-flexion in Choristodera (Fig. 11)

Angles of dorsi-flexion were estimated using Index 3 (Fig. 3F: difference between angle β_{post}° and β_{ant}°) for four species of *Champsosaurus* (*C. gigas*, *C. albertensis*, *C. laramiensis, C. natato*) and also for *Simoedosaurus dakotensis* at two possible pivot points as above, centre (β_{post1}°) and dorsal-most point (β_{post2}°) on the inter-cervical joint surface**.** In *Champsosaurus,* the estimated angles of dorsi-flexion are similar for both pivot points at less than 10º for most joints of the species examined, with *C. albertensis* being one of the exceptions (Fig 11A, B). *C. albertensis* is estimated to have been capable of greater flexibility in the anterior portion of the neck (e.g. V2/3 ~13–23º). This might be species specific, but the v2 and v3 of the specimen studied (RTMP 86.12.11) are connected by matrix and the lateral surfaces of the centra are not horizontal, which could be a source of error.

By contrast, estimates for the shorter-snouted *Simoedosaurus dakotensis* indicate similar values for the two pivot points (Fig 11C, D), and these results suggest a greater potential for dorsi-flexion (15–18º) in the anterior part of the neck (v2/v3), with more limited dorsi-flexion further posteriorly (> ~10°).

Discussion

Among slender snouted crocodilians, *Gavialis gangeticus* demonstrates a unique mechanism of lateral neck flexion that combines the following components: 1) anteroposterior elongation of vertebral centra, increasing the range of total neck movement; 2) lateral flexion mainly occurring anteriorly at v2/v3 (EZA, α = ~130°; ϕ_{lat}°, ~17.9°), v3/v4 (EZA, α = ~90°; ϕ_{lat}°, ~21.3°); and 3) a capacity for dorsi-flexion through v3–9, as indicated by Indices 3 [β_{post}°-β_{ant}°] and 4 [γ°], but dorsi-flexion occurring mainly at the v3/v4 and v4/v5 joints (15° –20° in [θ_{up}°]). Thus, the anterior part of the neck is most effective for lateral neck flexion to catch prey, and dorsi-flexion is essential for inertial feeding, as observed in *Gavialis gangeticus* (e.g. Gans 1969). Thorbjarnarson (1990) reported that many lateral strikes in *G. gangeticus* contain a vertical component that is accomplished by a rotation of up to 90° of the head and neck. This is consistent with the positional

changes in EZAs along the neck and the slight rotation about the antero-posterior axes of centra, especially through the cervical region during lateral flexion, as observed in the µCT reconstructions (Fig. 9D). The range of dorsi-flexion is large at all inter-cervical joints in short-snouted crocodilians (maximum angle of dorsi-flexion ~15°), which may also reflect their inertial feeding, a strategy that involves a sharp dorsal movement of the cranium and neck, (e.g. Cleuren & De Vree 1992).

In addition, the moment arm (M) of the dorsi-flexors relative to the whole neck (v2–9) length is small in *G. gangeticus* (Fig. 7A). This low value of the relative moment arm suggests the dorsi-flexor muscles may be less efficient at resisting cervical ventro-flexion induced by the weight of the skull or by struggling prey captured in the long jaws. The small moment arm of *G. gangeticus*, especially in the adult specimen (KPM-NFR 92: STL ~3 m), might reflect its more aquatic lifestyle, and a specialisation towards feeding on swallowable-sized fish, rather than attempting to tear pieces off larger prey.

The methods (Indices) tested to estimate joint flexibility from vertebral morphology in crocodilians, and validated by the µCT data, were then applied to neochoristoderes (*Champsosaurus* and *Simoedosaurus*). Neither *Champsosaurus* nor *Simoedosaurus* shows the vertebral elongation seen in *Gavialis gangeticus*. However, the cervical vertebrae of *Champsosaurus* are characterised by high EZAs (α = ~180°) in the middle to posterior neck (~v5/v6–v8/v9) (Index 1: EZA; Fig. 3A, B; Fig. 10), suggesting a very limited capacity for dorsi-flexion, a conclusion supported by the results of Index 3 examined from the two alternative pivot points ($\beta_{post}{}^{o}$-$\beta_{ant}{}^{o}$; Fig. 11A, B) which each yielded a value of less than 10°, except *C. albertensis* (possible error value). The horizontal zygapophysial facets (high EZA) imply that the posterior half of the neck is specialised for lateral flexion in the horizontal plane. *Simoedosaurus*, on the other hand, has fairly consistent EZAs (α = ~120°) throughout the neck, and is therefore interpreted to had been capable of combining lateral flexion with a dorsal component along the neck, rather than strictly horizontal movement. This action would be broadly similar to that of small short-snouted crocodilians (e.g. *Caiman latirostris*). Moreover, *Simoedosaurus* was estimated to have relatively

large angles of maximum dorsi-flexion ($\beta_{post}{}^{o}$-$\beta_{ant}{}^{o}$; 15° –20°) in the middle portion of the neck (v4-/v5, v5/v6: Fig. 11C, D). The middle to posterior cervical vertebrae of *Simoedosaurus* also bear an accessory spinous process below the post-zygapophyses (v6–8 in *S. dakotensis*; v5–9 in *S. lemoinei*). Given that these processes lie posterior to the maximum point of dorsi-flexion (v5/v6), they may have contacted the pre-zygapophyses of the succeeding cervical in the dorsi-flexed position, limiting further dorsi-flexion. Thus, the necks of *Champsosaurus* and *Simoedosaurus* show clear differences in the estimated range of lateral and dorsi-flexion, differences that might correlate with their feeding behaviour. On the other hand, the dorsi-flexor moment arms (Index 2) are similar in *Champsosaurus* and *Simoedosarus* (Fig. 7B), and these values are greater than those of *Gavialis gangeticus.* This result suggests that the necks of the two choristoderes have a greater potential to raise the head powerfully against gravity compared to *G. gangeticus,* and these reptiles may have been better in holding larger struggling prey in their jaws.

The slender-snouted *Gavialis* and *Champsosaurus* seem to be specialised for lateral neck flexion. However, they appear to differ in the position of maximum flexion: anteriorly in *Gavialis* and middle-posteriorly in *Champsosaurus*. The middle to posterior position of maximum lateral flexion in *Champsosaurus* may be correlated with restricted anterior neck mobility due to the postero-lateral expansion of the skull up to roughly the level of v3 (e.g. Brown 1905; Erickson 1972). Concomitant with lateral flexion of the anterior neck in *Gavialis,* there is weak rotation about a cranio-caudal axis through the cervical series. This complicated movement may be permitted by the procoelous vertebral joints. Although neck movement has not been simulated in *Champsosaurus*, the results of this study suggest that the amphiplatyan intercentral joints may have limited the potential for dorsolateral torsion. Another difference between *Champsosaurus* and *Gavialis* appears to be the capacity for neck dorsi-flexion, relatively high in *Gavialis*, especially in the middle part of the neck (v4–6: Fig. 6), and low or absent in *Champsosaurus* throughout the neck (Fig. 10). In combination, these results suggest that *Champsosaurus* is unlikely to have used inertial feeding. As in other choristoderes, *Champsosaurus* has an extensive palatal dentition consisting of longitudinal palatal

tooth rows and transverse pterygoid flange tooth rows (Matsumoto & Evans 2016). The orientation of the palatal tooth crowns changes with their position on the palate, supporting the view that they are involved in intra-oral food transportation, presumably in combination with a fleshy tongue (Matsumoto & Evans 2016). The secondary palate of crocodilians, as well as their tongue surface, is covered by keratinised epithelium forming rounded tubercles (Iwasaki 2002). The pattern of tubercles varies among taxa and may help to grip prey. For example, *Osteolaemus tetraspis*, which tends to eat hard prey such as crabs (Luiselli et al. 1999), has many large rounded papillae on the tongue, palate and the inner wall of the mandible. In contrast, the fish-eating *Gavialis* has a smooth palate and tongue, and keratinised papillae are only weakly developed (Matsumoto & Evans 2017). Thus, the size and distribution pattern of keratinised papillae may reflect prey texture. Hard prey must be firmly gripped in order to crush it, and the large papillae may prevent the prey slipping out of the mouth. Although fish are also slippery, they can slide easily into the pharynx once they are correctly positioned (fish head toward pharynx) and can be swallowed whole.

Short/ medium-snouted crocodilians are all similar to one another in general cervical morphology but the degree of dorsi-flexion, as reflected in the pattern of EZAs, varies among species, and might correspond to their different feeding behaviours (such as sideways strikes of the head, or a death roll using the whole body) and different prey types at the land-water interface (e.g. terrestrial mammals, birds, fish, amphibians; Gordon & Kirshner 2015). Among the crocodilians examined, the choristodere *Simoedosaurus* is most similar to small short-snouted crocodilians, such as *Caiman latirostris* and *Caiman crocodilus*, in having a relatively consistent value of EZA (α = ~120°) throughout the neck, suggestive of bilateral motion with some dorso-ventral range. The feeding behaviour of *Caiman latirostris* and *Caiman crocodilus* is little known. In the laboratory, *C. latirostris* has been reported to have a bottom scooping feeding behaviour (Diefenbach 1979), as observed in other crocodilians (Brazaitis 1969). *Caiman crocodilus,* mainly a piscivore, is reportedly an ambush hunter (Schaller & Crawshaw 1982). It lies in the shallows, on the bottom of ponds, or floats on the surface, and when prey reaches within snapping distance, the caiman either catches it

sideways or lunges forward with a half open mouth (Schaller & Crawshaw 1982). Whether, *Simoedosaurus* had a similar feeding behaviour cannot be determined. However, such strategies require a generalised dorsolateral neck mobility, which would be consistent with the cervical vertebral morphology of *Caiman* and possibly also of *Simoedosaurus*. In addition, a capacity for dorsi-flexion in *Simoedosaurus* might have allowed it to aim at terrestrial prey from under the water surface. The other role for dorsi-flexion would be inertial feeding as in crocodilians. However, *Simoedosaurus* has broad palatal tooth rows, corresponding to the greater snout width. These provided an efficient gripping surface for large prey and suggest tongue-driven intraoral transport (Matsumoto & Evans 2016). Taken together with the cervical morphology, *Simoedosaurus* is unlikely to have been an inertial feeder, and its shorter snout and shagreen of palatal teeth could have allowed it to grab and hold various types of prey, using generalised neck movements including dorsolateral sweeping. Evans & Hecht (1993) suggested that the morphological differences between the snouts of *Simoedosaurus* and *Champosaurus* might reflect their prey type and/or niche, and our results support that hypothesis from a different perspective.

This study focused on the potential for lateral and dorsi-flexion of the neck in crocodilians and choristoderes. Further work is planned using three-dimensional analyses like those employed herein to investigate the potential for rotation and ventral flexion, as well as the limitations imposed by the cervical ribs.

CONCLUSIONS

Gavialis gangeticus has often been used as eco-analogue of the extinct choristodere *Champsosaurus*, in terms of diet and feeding behavior. Both reptiles are specialised for lateral neck flexion but in different ways: in *Gavialis*, lateral flexion mainly occurs in the anterior neck, with a slight rotation about the cranio-caudal axis through the neck; in *Champsosaurus* horizontal lateral flexion is estimated to have occurred through the middle to posterior part of the neck, with

movement in the anterior neck constrained by the cordiform skull that extends posteriorly above the beginning of the neck.

Champsosaurus may have used its slender snout to grab fish from shoals using lateral sweeping motions of the neck, but inertial feeding is unlikely to have occurred and intraoral transport is likely to have combined a fleshy tongue working against the cranio-caudally aligned palatal dentition.

The choristodere *Simoedosaurus* may have had a wider range of neck movements with both dorsal and lateral components, a pattern broadly similar to that of small short-snouted crocodilians (e.g. *Caiman latirostris*). A capacity for dorsi-flexion of the neck may have allowed *Simoedosaurus* to grab prey above the water. Where the two choristoderes occurred in same place, they may have divided their niche by prey type.

ACKNOWLEDGEMENTS

We would like to thank M. Manabe and C. Sakata (National Museum of Nature and Science, Tokyo, Japan) for CT scanning; J. Hutchinson (Royal Veterinary College, UK) for creative comments and discussion; B. Erickson and J. Hoff (Science Museum Minnesota, USA), X-C. Wu and M. Feuerstack (Canadian Museum of Nature, Ottawa, Canada), M. Lowe (University Museum Cambridge, UK), A. Folie (Institut Royal des Sciences Naturelles de Belgique), J. Ashby and M. Carnall (formerly of Grant Museum of Zoology, UCL, London, UK), C. Barras (Natural History Museum, London, UK), R. Allain (Muséum National d'Histoire Naturelle, Paris, France), H. Endo (The University Museum, the University of Tokyo, Japan) for access to choristodere and extant crocodilian specimens; Hirakawa Zoo (Kagoshima Prefecture, Japan),T. Shirowa (iZoo, Shizuoka Prefecture, Japan); Atagawa Tropical & Alligator Garden (Shizuoka Prefecture, Japan), Nogeyama Zoo (Kanagawa Prefecture, Japan) for providing crocodilian specimens. The research was supported financially by the Estes Memorial Grant of the Society of Vertebrate Paleontology, the

Sasakawa Scientific Research Grant from the Japan Society, the Japan Society for the Promotion of Science Scholarship, Fujiwara Natural History Foundation, and the Japan Society for the Promotion of Science Scholarship (JSPS) KAKENHI Grant Number 17K05698. We also grateful to two reviewers for their helpful comments to improve an earlier version of the manuscript.

REFERENCES

Brazaitis P (1969) The occurrence and ingestion of gastroliths in two captive crocodilians. *Herpetologica* **25**, 63–64.

Brochu CA (2001) Crocodylian snouts in space and time: phylogenetic approaches toward adaptive radiation. *Am Zool* **41**, 564–585.

Brown B (1905) The osteology of *Champsosaurus* Cope. *Am Mus Nat Hist Mem* **9**, 1–26.

Busbey AB (1995) The structural consequences of skull flattening in crocodilians. In: *Functional Morphology in Vertebrate Paleontology*. (ed. Thomason JJ), pp. 173–192. Cambridge: Cambridge University Press.

Cleuren J, De Vree F (1992) Kinematics of the jaw and hyolingual apparatus during feeding in *Caiman crocodilus*. *J Morphol* **212**, 141–154.

Diefenbach COC (1979) Ampullarid gastropod-staple food of *Caiman latirostris*? *Copeia* **1**, 162–163.

Dilkes DW (1998) The early Triassic rhynchosaur *Mesosuchus browni* and the interrelationships of

basal archosauromorph reptiles. *Philos Trans R Soc London Ser B* **353**, 501–541.

Efimov MB (1975) Khampsosaurid iz nizhnego mela Mongolii [A champsosaurid from the Lower Cretaceous of Mongolia]. *Tr Sovmest Sov Mong Paleontol Eksped* **2**, 84–94.

Erickson BR (1972) The lepidosaurian reptile *Champsosaurus* in North America. *Sci Mus Minn Monogr (Paleontol)* **1**, 1–91.

Erickson BR (1985) Aspects of some anatomical structures of *Champsosaurus* (Reptilia: Eosuchia). *J Vertebr Paleontol* **5**, 111–127.

Erickson BR (1987) *Simoedosaurus dakotensis,* new species, a diapsid reptile (Archosauromorpha: Choristodera) from the Paleocene of North America. *J Vertebr Paleontol* **7**, 237–251.

Evans AR, Sanson GD (1998) The effect of tooth shape on the breakdown of insects. *J Zool* **246**, 391–400.

Evans SE (1990) The skull of *Cteniogenys*, a choristodere (Reptilia: Archosauromorpha) from the Middle Jurassic of Oxfordshire. *Zool J Linn Soc* **99**, 205–237.

Evans SE, Hecht MK (1993) A history of an extinct reptilian clade, the Choristodera: longevity, Lazarus-taxa, and the fossil record. *Evol Biol* **27**, 323–338.

Evans SE, Manabe M (1999) A choristoderan reptile from the Lower Cretaceous of Japan. *Spec Pap Palaeontol* **60**, 101–119.

Fish FE, Bostic SA, Nicastro AJ, Beneski JT (2007) Death roll of the alligator: mechanics of twist feeding in water. *J Exp Biol* **210**, 2811–2818.

Fox RC (1968) Studies of Late Cretaceous vertebrates I: The braincase of *Champsosaurus* Cope (Reptilia: Eosuchia). *Copeia* **1968**, 100–109.

Fronimos JA, Wilson JA (2017) Concavo-convex intercentral joints stabilize the vertebral column in sauropod dinosaurs and crocodylians. *Ameghiniana* 54, 151–176.

Gans C (1969) Comments on inertial feeding. *Copeia* **4**, 855–857.

Gao K, Evans SE, Ji Q, Norell M, Ji S (2000) Exceptional fossil material of a semi-aquatic reptile from China: the resolution of an enigma. *J Vertebr Paleontol* **20**, 417–421.

Gignac PM, O'Brien HD, Turner AH, Erickson GM (2019) Feeding in crocodylians and their relatives: functional insights from ontogeny and evolution. In: *Feeding in Vertebrates*. (eds. Bels V, Whishaw IQ), pp. 575–610. Springer Nature Switzerland AG.

Gordon G, Kirshner D (2015) *Biology and Evolution of Crocodylians*. pp 649. Cornell University Press Ithaca and London.

Hoffstetter R, Gasc JP (1969) Vertebrae and ribs of modern reptiles. In: *Biology of the Reptilia 1*, (ed. Gans, C), pp. 201–310. Academic Press, London.

Hua S (2003) Locomotion in marine mesosuchians (Crocodylia): the contribution of the "locomotion profiles" *N. Jb Geol Paläont Abh* **22**,139–152.

Iijima M, Kubo T (2019) Comparative morphology of presacral vertebrae in extant crocodylians: taxonomic, functional and ecological implications. *Zool J Linn Soc* **186**, 1006–1025.

Iwasaki S (2002) Evolution of the structure and function of the vertebrate tongue. *J Anat* **201**, 1–13.

Kowalski JR, Ferrara LA, Benzel EC (2005) Biomechanics of the spine. *Neurosurg* **15**, 42–59.

Langston W (1973) The crocodilian skull in historical perspective. In: *Biology of the Reptilia 4, Morphology D.* (eds. Gans C, Bellairs A, Parsons TS), pp. 263–284. Academic Press, London.

Long JH, Pabst Jr DA, Shepherd WR, McLellan WA (1997) Locomotor design of dolphin vertebral columns: bending mechanics and morphology of *Delphinus delphis*. *J Exp Biol* **200**, 65–81.

Luiselli L, Akani GC, Capizzi D (1999) Is there any interspecific competition between dwarf crocodiles (*Osteolaemus tetraspis*) and Nile monitors (*Varanus niloticus ornatus*) in the swamps of central Africa? A study from south-eastern Nigeria. *J Zool* **247**, 127–131.

Massare, JA 1987. Tooth morphology and prey preference of Mesozoic marine reptiles. *J Vertebr Paleontol* **7**, 121–137.

Matsumoto R (2011) The Palaeobiology of Choristodera (Reptilia: Diapsida). PhD Thesis, University College London, UK, 437 pp.

Matsumoto R, Buffetaut E, Escuillie F, Hervet S, Evans SE (2013) New material of the choristodere *Lazarussuchus* (Diapsida, Choristodera) from the Paleocene of France. *J Vertebr Paleontol* **33**, 319–339.

Matsumoto R, Evans SE (2010) Choristoderes and the freshwater assemblages of Laurasia. *J Iber Geol* **36**, 253–274.

Matsumoto R, Evans SE (2016) Morphology and function of the palatal dentition in Choristodera. *J Anat* **228**, 414–429.

Matsumoto R, Evans SE (2017) The palatal dentition of tetrapods and its functional significance. *J Anat* **230**, 47–65.

Molnar JL, Pierce SE, Hutchinson JR (2014) An experimental and morphometric test of the relationship between vertebral morphology and joint stiffness in Nile crocodiles (*Crocodylus niloticus*). *J Exp Biol* **217**, 758–768.

Molnar JL, Pierce SE, Bhullar B-AS, Turner AH, Hutchinson JR (2015) Morphological and functional changes in the vertebral column with increasing aquatic adaptation in crocodylomorphs. *R Soc Open Sci* **2**, 150439.

Mook CC (1921) Skull characters of recent Crocodilia: with notes on the affinities of the recent genera. *Bull Am Mus Nat Hist* **44**,123–268.

Neenan JM, Klein N, Scheyer TM (2013) European origin for sauropterygian marine reptiles and the evolution of placodont crushing dentition. *Nat Commun* **4**, 1621.

Neill WT (1971). *The last of the ruling reptiles; alligators, crocodiles, and their kin*. 6th Edition. pp. 486. Columbia University Press, New York.

Pierce SE, Clack JA, Hutchinson JR (2011). Comparative axial morphology in pinnipeds and its correlation with aquatic locomotory behaviour. *J Anat* **219**, 502–514.

Pooley AC, Gans C (1976) The Nile crocodile. *Sci Am* **234**: 114–124.

Schaller GB, Crawshaw PG Jr (1982) Fishing behavior of Paraguayan caiman (*Caiman crocodilus*). *Copeia* **1982**, 66–72.

Shapiro L (1995) Functional morphology of indrid lumbar vertebrae. Am *J Phys Anthropol* **98**, 323–342.

Sigogneau-Russell D, Russell, DE (1978) Étude ostéologique du Reptile *Simoedosaurus* (Choristodera). *Ann Paléontol (Vertébrés)* **64**, 1–84.

Taylor MA (1987) How tetrapods feed in water: a functional analysis by paradigm. *Zool J Linn Soc* **91**, 171–195.

Thorbjarnarson J (1990) Notes on the feeding behavior of the Gharial (*Gavialis gangeticus*) under semi–natural conditions. *J Herpetol* **24**, 99–100.

928

929 **FIGURE CAPTIONS**

930 Fig.1 Morphological variation in the skull of Choristodera and Crocodylia; A) *Simoedosaurus*
931 *dakotensis* (SMM P76.10.1); B, *Simoedosaurus lemoinei* (after Sigogneau-Russell & Russell,
932 1978); C, *Tchoiria namusarai* (after Efimov, 1975); D, *Ikechosaurus sunailinae* (IVPP V9611-1); E,
933 *Champsosaurus gigas* (after Erickson, 1985); F, *Osteolaemus tetraspis*; G, *Alligator*
934 *mississippiensis*; H, *Crocodylus acutus*; I, *Tomistoma schlegelii*; J, *Gavialis gangeticus*.

935

936 Fig. 2 Morphologically informative measurements; left lateral views of vertebrae in choristoderes (as
937 represented by *Champsosaurus gigas*) (A) and crocodilians (as represented by *Alligator*
938 *mississippiensis*) (B); sagittal section of vertebrae in crocodilians (C) (as represented by *Gavialis*
939 *gangeticus*). Vertebral measurements used in this study: CH, centrum height; CL, craniocaudal
940 length of the centrum along the vertebral margin; NH, neural spine (ns) height. The ventral axis of
941 the centrum is almost parallel to the floor of the neural canal as shown in sagittal section (C).

942

943 Fig. 3 Biomechanically informative measurements; anterior (A) and posterior (B) views of vertebrae
944 in choristodderes (as represented by *Simoedosaurus dakotensis*). Vertebral measurements used in
945 this study: EZAa/ EZAp, enclosed pre- and post-zygapophyseal angles (A, B: Index 1). Lateral
946 views of vertebrae in choristoderes (C) and crocodilians (D) (same species as in Fig. 2); distance
947 from the pivot of the inter-central joint to the distal-most point of the neural spine using centrum
948 height (CH) and neural spine height (NH) (C, D: Index 2). Orientation of pre-zygapophysis for dorsi-
949 flexion, estimated maximum dorsi-flexion angles are provided by the difference between angle β_{post}
950 and β_{ant} [°] in crocodilians (E: Index 3); orientation of pre-zygapophysis for dorsi-flexion, estimated
951 from two pivot point positions, centre of centrum (1) and the dorsal-most point on the inter-cervical
952 joint (2) in choristoderes (F: Index 3); diagram of the maximum inter-cervical dorsi-flexion angles
953 shown as "γ [°]" (G: Index 4).

954

955 Fig. 4 μCT images of three cervical postures in *Gavialis gangeticus* (KPM-NFR 52; A–D) used in
956 the validation studies; Standard posture, the skull in neutral position in left lateral view (A); Upward
957 posture, the skull in maximum dorsi-flexed position seen in left lateral view (B); Lateral-flexed
958 posture, the skull in laterally directed position, in dorsal view (C).

959

960

961 Fig. 5 Functional relevance of cervical measurements with results of comparison. The cervical
962 vertebrae of a single individual are connected by solid lines from v2–9 in the graph. X axis: centrum
963 length/ centrum height (CL/CH); Y axis neural spine height/ centrum height (NH/CH).
964 Abbreviations for each specimen are given in Supplementary Table 1.

965

966

967 Fig. 6 Positional change of the enclosed zygapophysial angles (EZA) in Crocodylia for each taxon.
968 The diagram shows positional changes in the enclosed zygapophyseal angle along the neck (v2–9).
969 A, *Gavialis gangeticus* (KPM-NFR 18, 52, 92); B, *Tomistoma schlegelii* (KPM-NFR 64; UMUT
970 12279); C, *Alligator mississippiensis* (KPM-NFR 16, 109); D, *Caiman latirostris* (KPM-NFR 54, 84).

971

972 Fig. 7 Values of dorsi-flexor moment arms in relation to the total neck length in Crocodylia (A), and
973 Choristodera (B). In choristoderes, two possible pivot points were used: maximum moment arm
974 (M_1), at the centre of the centrum of the inter-central joint; minimum moment arm (M_2), at the dorsal-
975 most point of the inter-central joint.

976

977 Fig. 8 Plots of estimated and in situ angles of dorsi-flexion in the joints of v2–9 in: A, *Gavialis*
978 *gangeticus* (KPM-NFR 52); B, *Caiman latirostris* (KPM-NFR 54). Maximum inter-cervical angle of
979 lateral flexion *in situ* in: C, *Gavialis gangeticus* (KPM-NFR 52); D, *Caiman latirostris* (KPM-NFR 54).

(1) Index 3, estimated maximum angle of dorsi-flexion (β_{post}°-β_{ant}°); (2) Index 4, estimated maximum angle of dorsi-flexion (γ°); (3) Standard posture, angle of dorsi-flexion measured *in situ* from μCT (θ_{st}°); (4) Upward posture, angle of dorsi-flexion measured *in situ* from μCT (θ_{up}°); (5) Lateral-flexed posture, angle of dorsi-flexion measured in situ from μCT (θ_{lat}°); (6) Standard posture, angle of lateral-flexion measured *in situ* from μCT (ϕ_{st}°); (7) Upward posture, angle of lateral flexion measured *in situ* from μCT (ϕ_{up}°); (8) Lateral posture, angle of lateral flexion measured *in situ* from μCT (ϕ_{lat}°). The background colours in the graph corresponds to EZA (α); green α= 90º–135º; yellow α = 45º–90º.

Fig. 9 μCT image of *Gavialis gangeticus* (KPM-NFR 52; A–D) and *Caiman latirostris* (KPM-NFR 54; E–H) showing (in B, C) the relationship between the cervical vertebrae and the overlying osteoderms (light blue: ost) and pectoral girdle (dark blue) coracoid (co), scapula (sc) and humerus (hu); Standard neck posture in left lateral view (A, E); Upward neck posture in left lateral view (B, F); Lateral-flexed posture in ventral view (C, G); Lateral-flexed posture in antero-lateral view (D, H).

Fig. 10 Positional change of the Enclosed zygapophysial angles (EZA) in Choristodera; A, *Champsosaurus*; B, *Simoedosaurus*. For each taxon, the diagram shows positional changes in EZA along the neck (v2–9).

Fig. 11 Angles of dorsi-flexion at each intervertebral joint along the neck as estimated from two pivot points for Index 3. Dorsi-flexion angle 1, as the pivot point at the centre of the inter-central joint (β_{post1}°-β_{ant1}°), in *Champsosaurus* (A) and *Simoedosaurus* (C); Dorsi-flexion angle 2, as the pivot point at the dorsal-most point of the centrum (β_{post2}°-β_{ant2}°), in *Champsosaurus* (B) and *Simoedosaurus* (D).

Supplementary TABLE CAPTIONS

Table S1. List of choristoderan and extant crocodilian specimens used in this study.

Table S2. The angles of inter-cervical torsion, dorsi-flexion (θ°), and lateral flexion (ϕ°) angles *in vivo* measured for *Gavialis gangeticus* (KPM-NFR 52) and *Caiman latirostris* (KPM-NFR 54) specimens CT-scanned in the Straight (st), Upward (up), and Laterally-flexed (lat) neck postures.

Supplementary Figures

Supp. Fig. S1 Methodology used to measure the orientation of each cervical element in *Caiman latirostris* (KPM-NFR 54); A, cervical vertebrae (v2–9) in three different neck postures (Straight, Upward, and Lateral-flexed) are shown. The arrows in "A" indicate the unit-vectors of cranio-caudal (red), dorso-ventral (blue), and medio-lateral (green) axes of the ninth cervical (v9); B, an isolated cervical vertebra (e.g., third cervical [v3]) is labelled with the three unit-vectors; and C, the vertebra with the unit-vectors (e.g., v3) was superimposed onto its relevant *in situ* position in the neck for the three different neck postures, respectively. The inter-cervical joint angles were estimated using the unit-vectors of each consecutive pair of cervical vertebrae.

Supp. Fig. S2 Inter-cervical articulation angles *in situ* taken from fresh specimens of *Gavialis gangeticus* used for validation. Standard and Upward neck postures examined in left lateral view (A); Lateral-flexed neck posture examined in ventral view (B). The same method was used for *Caiman latirostris*.

Supp. Fig. S3 *Champsosaurus gigas* (SMM P 77.33.24) cervical vertebrae v1–9: A, in dorsal; B, in anterior; C, in left lateral views. Abbreviations: pc AT, pleurocentrum of atlas; ic AX, inter-centrum of axis; dp, diapophysis; pa, parapophysis; ri, ridge.

Supp. Fig. S4 *Simoedosaurus dakotensis* (SMM P 76.10.1) cervical vertebrae v1–8: A, in dorsal; B, in anterior; C, in lateral views. Abbreviations: dp diapophysis; f. ic AX; facet for inter-centrum of axis; ic AT, inter-centrum of atlas; ic AX, inter-centrum of axis; na AT, neural arch of atlas; pa, parapophysis; pl AX, pleurocentrum of axis; sp, spinous process.

Supp. Fig. S5 *Gavialis gangeticus* (KPM-NFR 18) cervical vertebrae v1–9; A, in anterior; B, in left lateral; C, in posterior views. Abbreviations are the same as in Figure S4.

Supp. Fig. S6 *Alligator mississippiensis* (KPM-NFR 16) cervical vertebrae v1–9; A, in anterior; B, in left lateral; C, in posterior views. Abbreviations are the same as in Figure S3.

Supp. Fig. S7 Positional change of the Enclosed zygapophysial angles (EZA) in Crocodylia. The diagram shows positional changes in EZA along the neck (v2–9) for each taxon. A, *Crocodylus acutus* (Mook, 1921); B, *Crocodylus niloticus* (UMUT 12260); C, *Osteolaemus tetraspis* (KPM-NFR 110; UMZC R 6286); D, *Alligator sinensis* (UMUT 12255); E, *Caiman crocodilus* (NSM-PO 421, 425); F, *Paleosuchus palpebrosus* (UMUT 13041).

Supp. Fig. S8 Angle of inter-cervical dorsi-flexion of v2–9, estimated from Indices 3 (β_{post}°-β_{ant}°) and 4 (γ°); A, *Gavialis gangeticus* (KPM-NFR 18); B, *Gavialis gangeticus* (KPM-NFR 92); C, *Tomistoma schlegelii* (UMUT 12779); D, *Alligator mississippiensis* (KPM-NFR 109); E, *Alligator mississippiensis* (KPM-NFR 16); F, *Alligator sinensis* (UMUT 12255); G, *Caiman crocodilus* (NSM-PO 421); H, *Crocodylus niloticus* (UMUT 12260); I, *Osteolaemus tetraspis* (KPM-NFR 110); J, *Paleosuchus palpebrosus* (UMUT 13041).

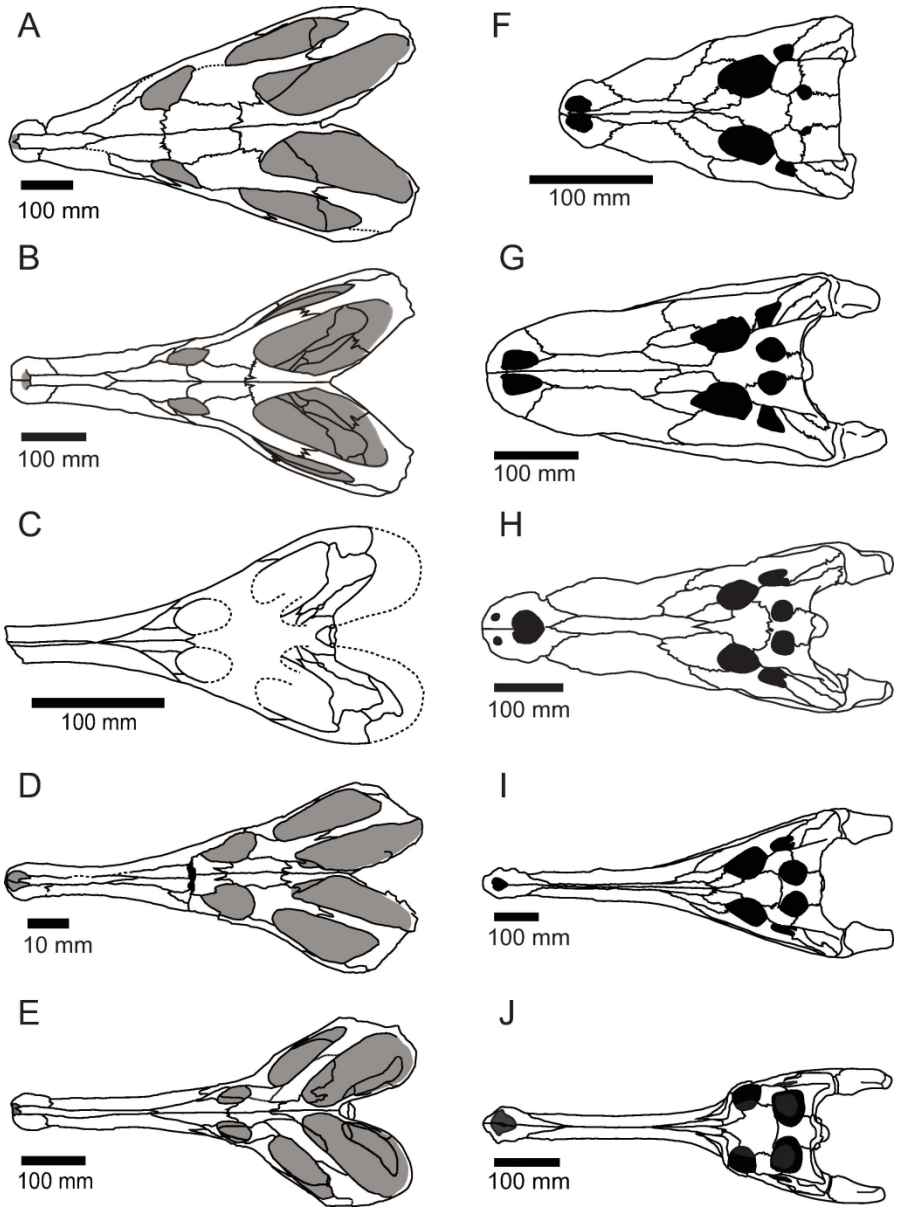

Fig.1 Morphological variation in the skull of Choristodera and Crocodylia; A) *Simoedosaurus dakotensis* (SMM P76.10.1); B, *Simoedosaurus lemoinei* (after Sigogneau-Russell & Russell, 1978); C, *Tchoiria namusarai* (after Efimov, 1975); D, *Ikechosaurus sunailinae* (IVPP V9611-1); E, *Champsosaurus gigas* (after Erickson, 1985); F, *Osteolaemus tetraspis*; G, *Alligator mississippiensis*; H, *Crocodylus acutus*; I, *Tomistoma schlegelii*; J, *Gavialis gangeticus*.

108x146mm (600 x 600 DPI)

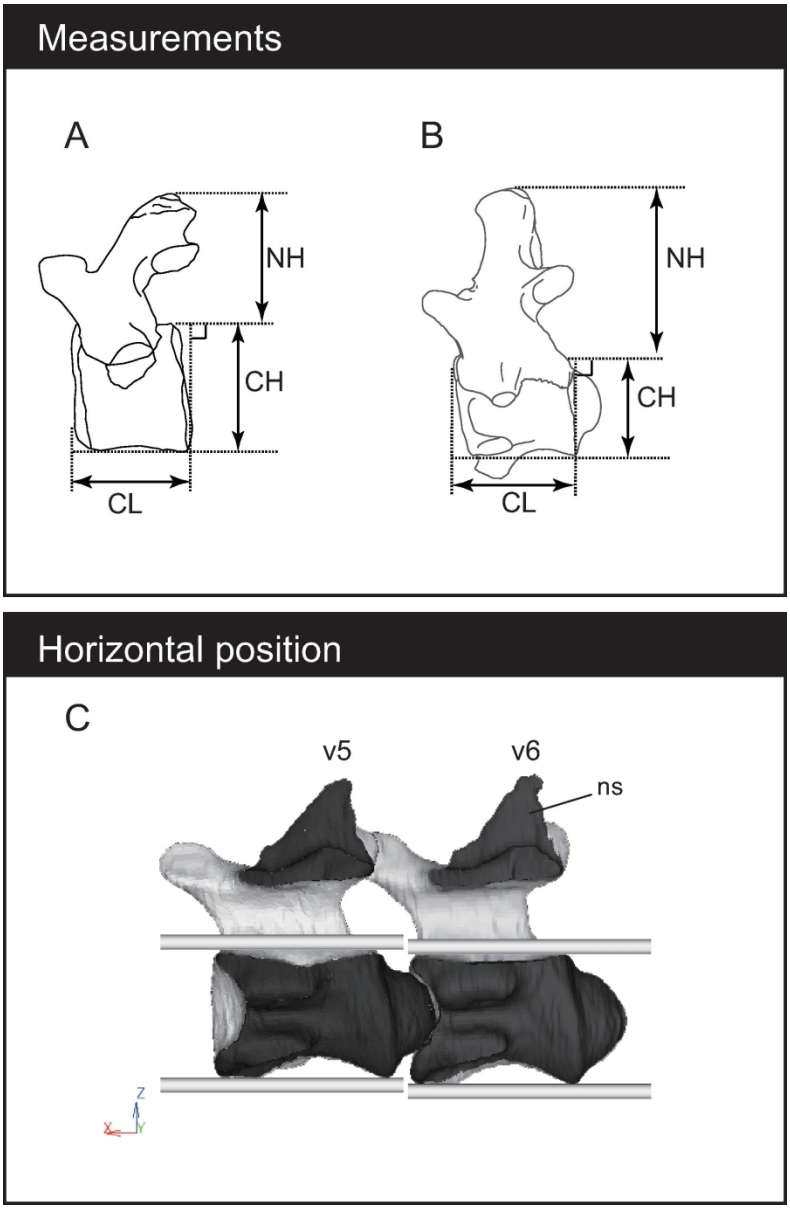

Fig. 2 Morphologically informative measurements; left lateral views of vertebrae in choristoderes (as represented by *Champsosaurus gigas*) (A) and crocodilians (as represented by *Alligator mississippiensis*) (B); sagittal section of vertebrae in crocodilians (C) (as represented by *Gavialis gangeticus*). Vertebral measurements used in this study: CH, centrum height; CL, craniocaudal length of the centrum along the vertebral margin; NH, neural spine (ns) height. The ventral axis of the centrum is almost parallel to the floor of the neural canal as shown in sagittal section (C).

89x136mm (600 x 600 DPI)

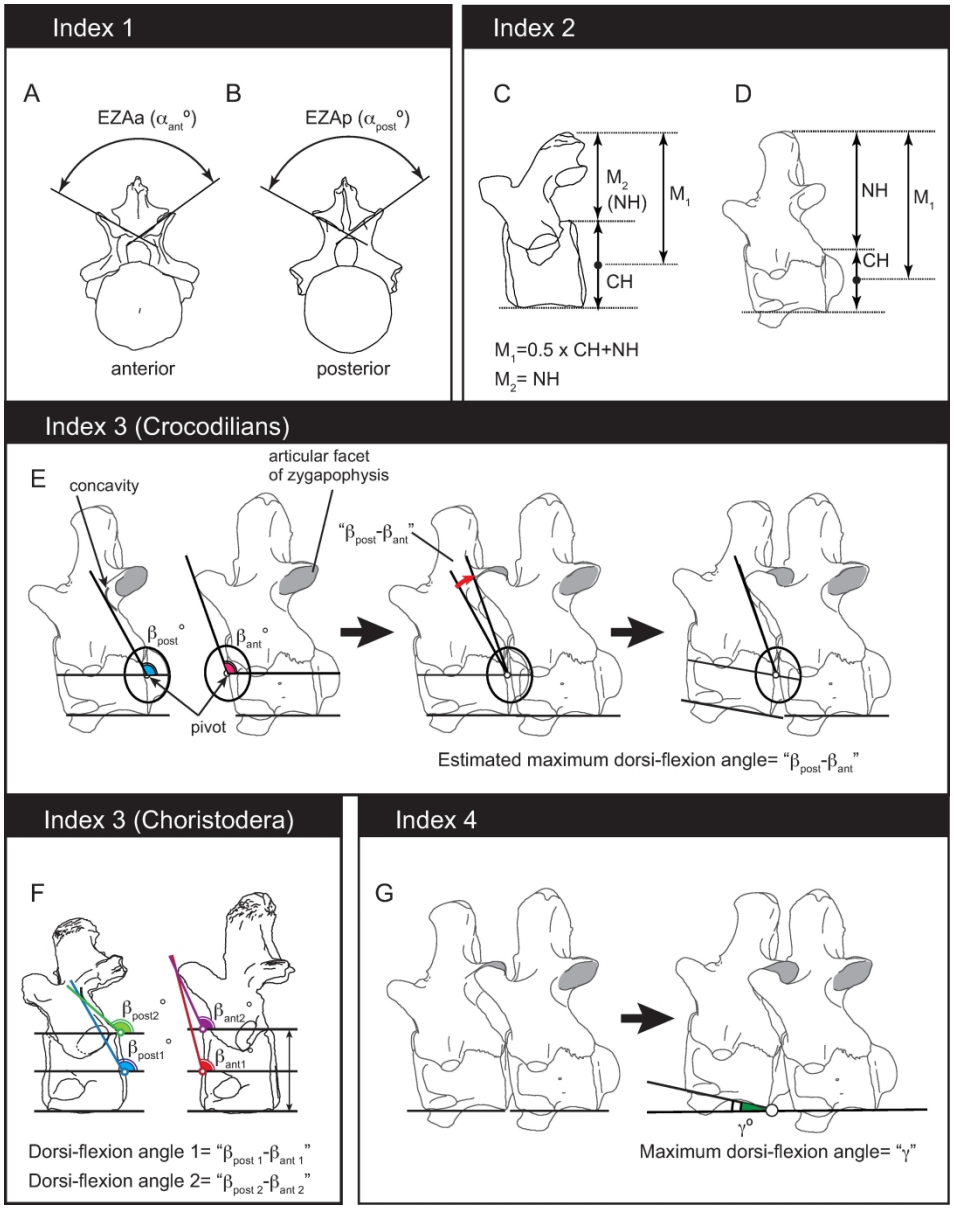

Fig. 3 Biomechanically informative measurements; anterior (A) and posterior (B) views of vertebrae in choristodderes (as represented by *Simoedosaurus dakotensis*). Vertebral measurements used in this study: EZAa/ EZAp, enclosed pre- and post-zygapophyseal angles (A, B: Index 1). Lateral views of vertebrae in choristoderes (C) and crocodilians (D) (same species as in Fig. 2); distance from the pivot of the inter-central joint to the distal-most point of the neural spine using centrum height (CH) and neural spine height (NH) (C, D: Index 2). Orientation of pre-zygapophysis for dorsi-flexion, estimated maximum dorsi-flexion angles are provided by the difference between angle β_{post} and β_{ant} [°] in crocodilians (E: Index 3); orientation of pre-zygapophysis for dorsi-flexion, estimated from two pivot point positions, centre of centrum (1) and the dorsal-most point on the inter-cervical joint (2) in choristoderes (F: Index 3); diagram of the maximum inter-cervical dorsi-flexion angles shown as "γ [°]" (G: Index 4).

159x201mm (600 x 600 DPI)

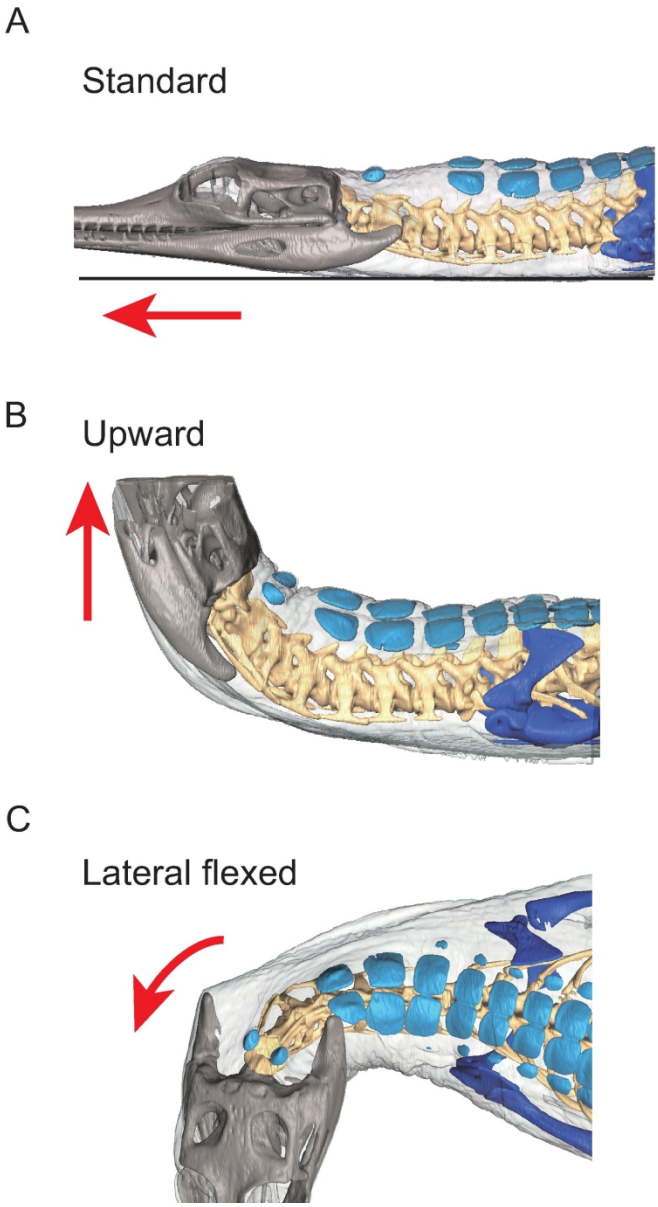

Fig. 4 µCT images of three cervical postures in *Gavialis gangeticus* (KPM-NFR 52; A–D) used in the validation studies; Standard posture, the skull in neutral position in left lateral view (A); Upward posture, the skull in maximum dorsi-flexed position seen in left lateral view (B); Lateral-flexed posture, the skull in laterally directed position, in dorsal view (C).

85x140mm (600 x 600 DPI)

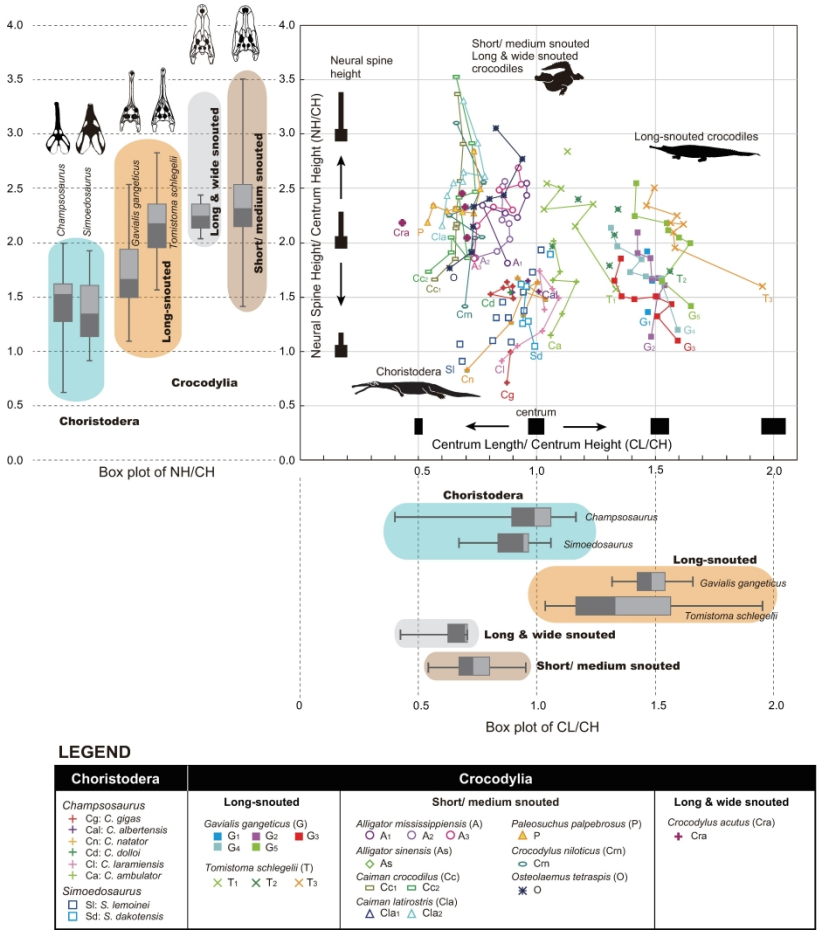

Fig. 5 Functional relevance of cervical measurements with results of comparison. The cervical vertebrae of a single individual are connected by solid lines from v2–9 in the graph. X axis: centrum length/ centrum height (CL/CH); Y axis neural spine height/ centrum height (NH/CH).
Abbreviations for each specimen are given in Supplementary Table 1.

222x296mm (600 x 600 DPI)

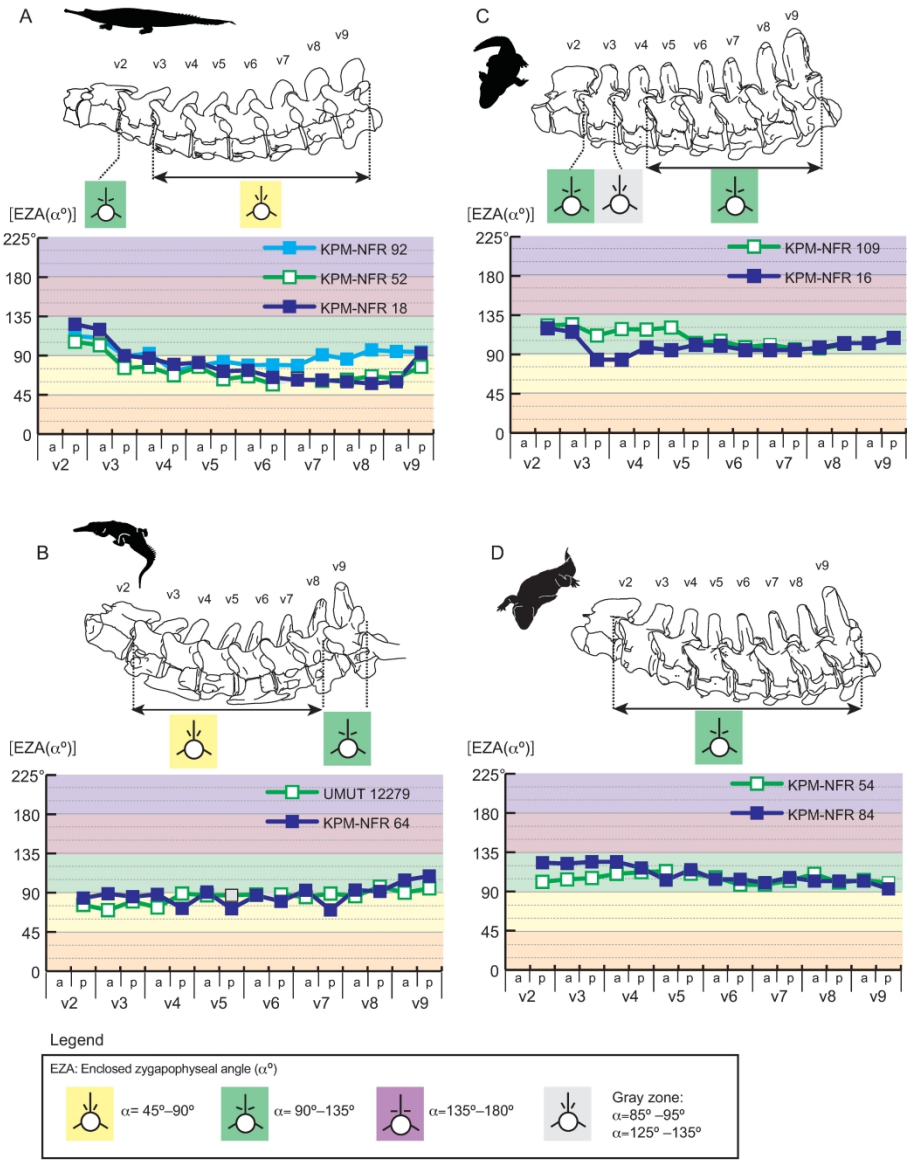

Fig. 6 Positional change of the enclosed zygapophysial angles (EZA) in Crocodylia for each taxon. The diagram shows positional changes in the enclosed zygapophyseal angle along the neck (v2–9). A, *Gavialis gangeticus* (KPM-NFR 18, 52, 92); B, *Tomistoma schlegelii* (KPM-NFR 64; UMUT 12279); C, *Alligator mississippiensis* (KPM-NFR 16, 109); D, *Caiman latirostris* (KPM-NFR 54, 84).

196x260mm (600 x 600 DPI)

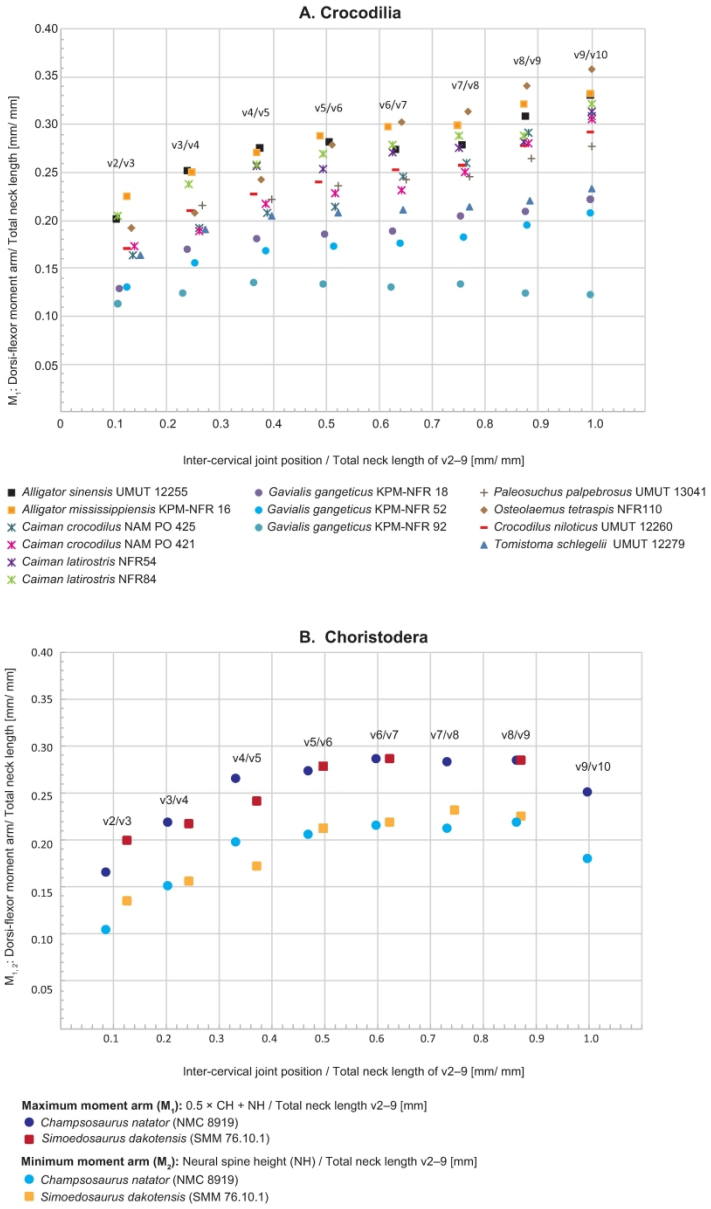

Fig. 7 Values of dorsi-flexor moment arms in relation to the total neck length in Crocodylia (A), and Choristodera (B). In choristoderes, two possible pivot points were used: maximum moment arm (M_1), at the centre of the centrum of the inter-central joint; minimum moment arm (M_2), at the dorsal-most point of the inter-central joint.

164x280mm (600 x 600 DPI)

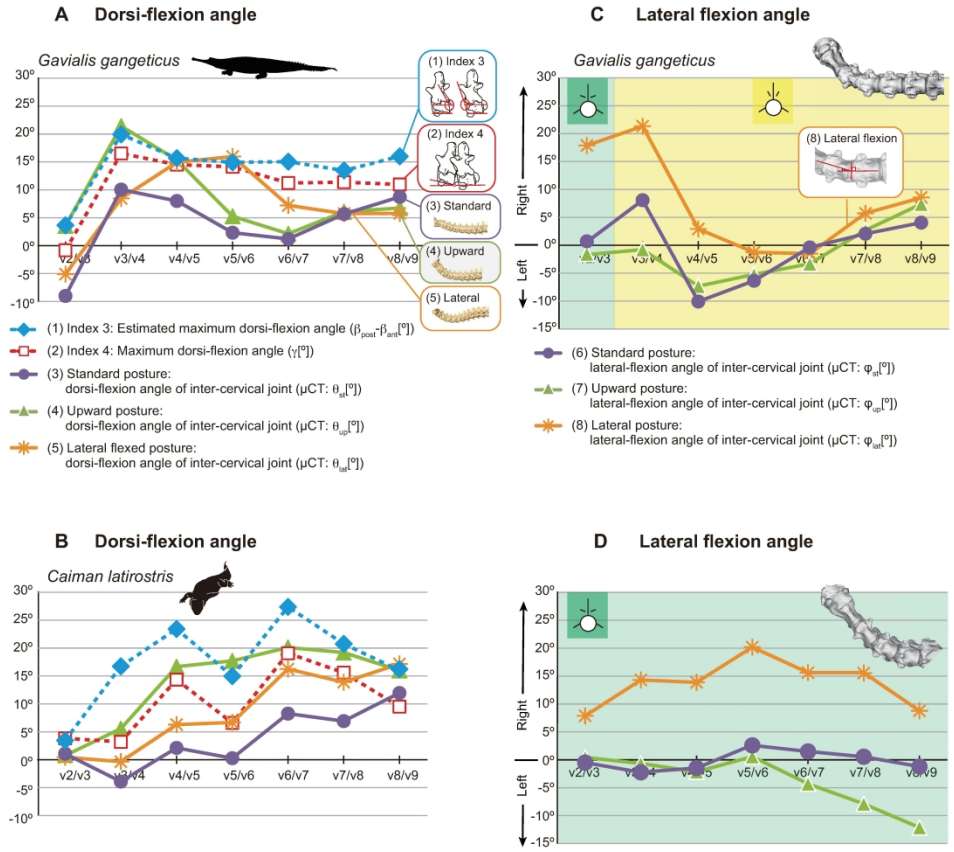

Fig. 8 Plots of estimated and in situ angles of dorsi-flexion in the joints of v2–9 in: A, *Gavialis gangeticus* (KPM-NFR 52); B, *Caiman latirostris* (KPM-NFR 54). Maximum inter-cervical angle of lateral flexion in situ in: C, *Gavialis gangeticus* (KPM-NFR 52); D, *Caiman latirostris* (KPM-NFR 54). (1) Index 3, estimated maximum angle of dorsi-flexion ($\beta_{post}°$-$\beta_{ant}°$); (2) Index 4, estimated maximum angle of dorsi-flexion (γ°); (3) Standard posture, angle of dorsi-flexion measured *in situ* from μCT ($\theta_{st}°$); (4) Upward posture, angle of dorsi-flexion measured in situ from μCT ($\theta_{up}°$); (5) Lateral-flexed posture, angle of dorsi-flexion measured in situ from μCT ($\theta_{lat}°$); (6) Standard posture, angle of lateral-flexion measured in situ from μCT ($\Phi_{st}°$); (7) Upward posture, angle of lateral flexion measured in situ from μCT ($\Phi_{up}°$); (8) Lateral posture, angle of lateral flexion measured in situ from μCT ($\Phi_{lat}°$). The background colours in the graph corresponds to EZA (α); green α= 90º–135º; yellow α = 45º–90º.

214x182mm (600 x 600 DPI)

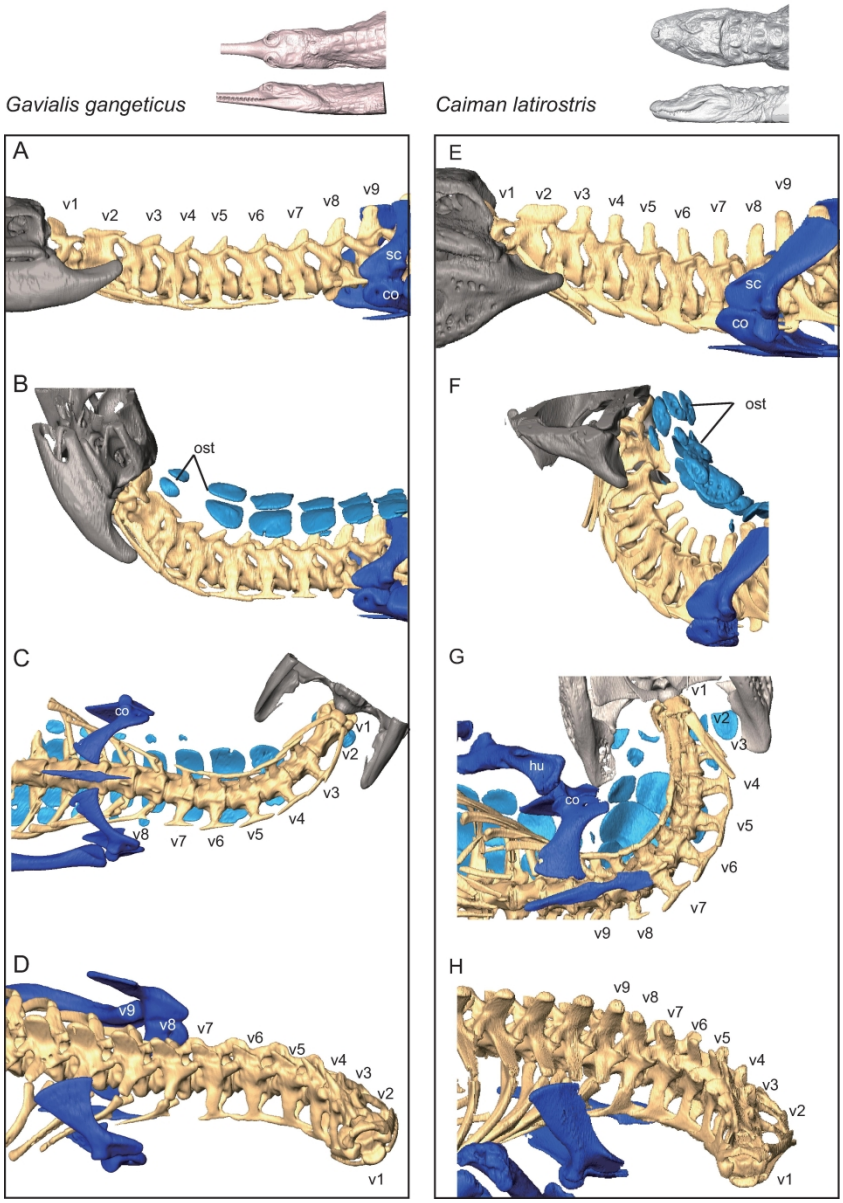

Fig. 9 µCT image of *Gavialis gangeticus* (KPM-NFR 52; A–D) and *Caiman latirostris* (KPM-NFR 54; E–H) showing (in B, C) the relationship between the cervical vertebrae and the overlying osteoderms (light blue: ost) and pectoral girdle (dark blue) coracoid (co), scapula (sc) and humerus (hu); Standard neck posture in left lateral view (A, E); Upward neck posture in left lateral view (B, F); Lateral-flexed posture in ventral view (C, G); Lateral-flexed posture in antero-lateral view (D, H).

169x243mm (600 x 600 DPI)

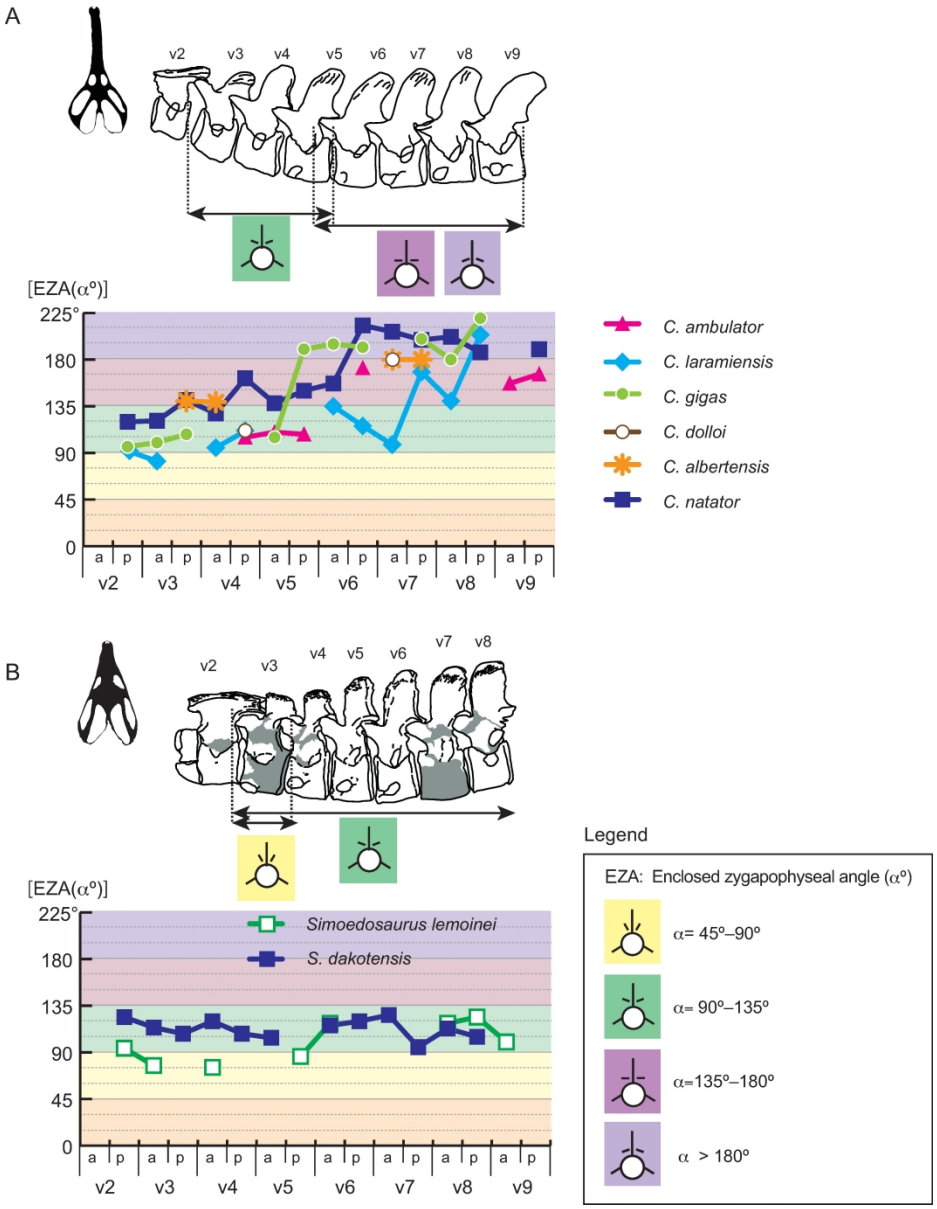

Fig. 10 Positional change of the Enclosed zygapophysial angles (EZA) in Choristodera; A, *Champsosaurus*; B, *Simoedosaurus*. For each taxon, the diagram shows positional changes in EZA along the neck (v2–9).

169x218mm (600 x 600 DPI)

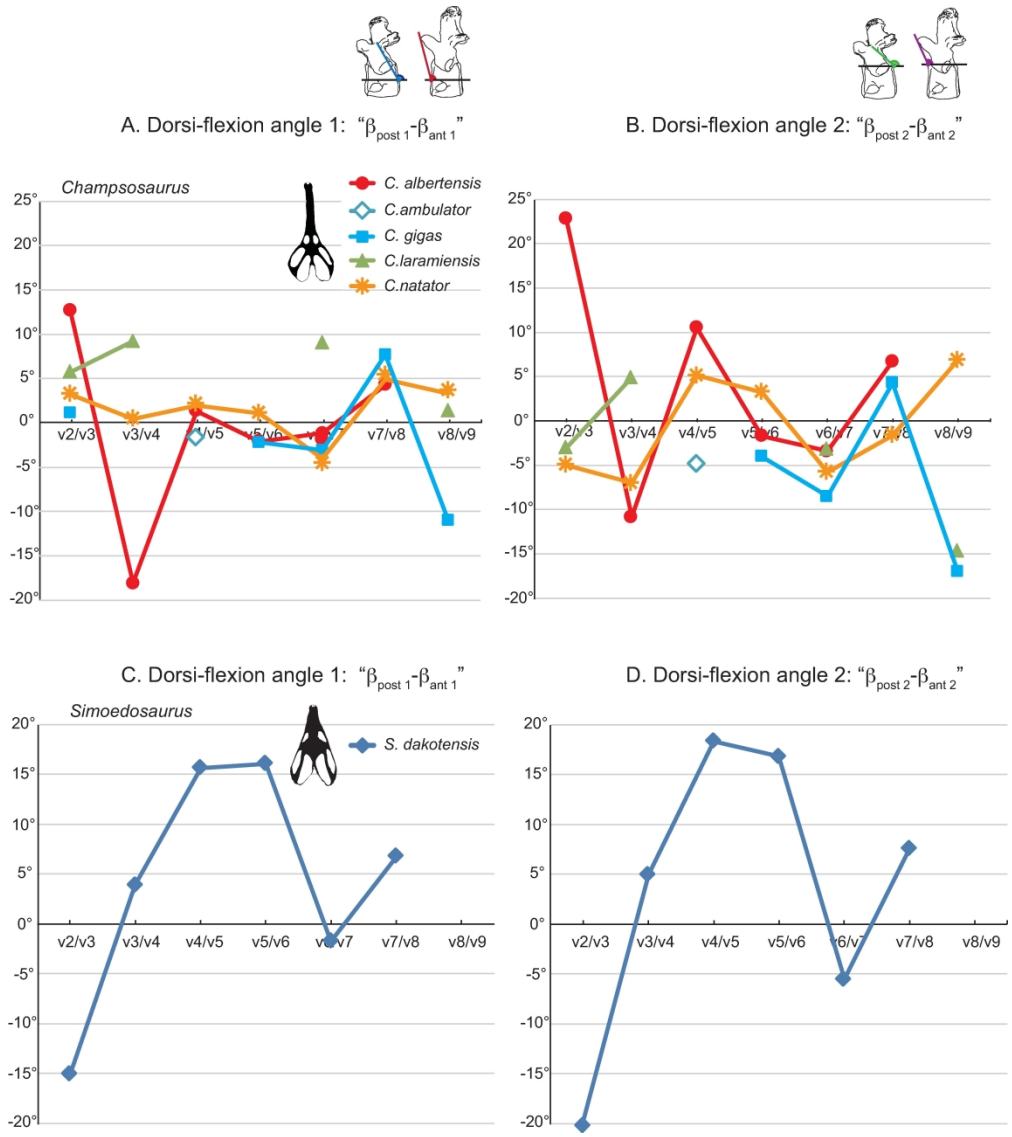

Fig. 11 Angles of dorsi-flexion at each intervertebral joint along the neck as estimated from two pivot points for Index 3. Dorsi-flexion angle 1, as the pivot point at the centre of the inter-central joint ($\beta_{post1}°$-$\beta_{ant1}°$), in *Champsosaurus* (A) and *Simoedosaurus* (C); Dorsi-flexion angle 2, as the pivot point at the dorsal-most point of the centrum ($\beta_{post2}°$-$\beta_{ant2}°$), in *Champsosaurus* (B) and *Simoedosaurus* (D).

199x224mm (600 x 600 DPI)

Taxa	Snout shape			Specimen No.
Choristodera	Long	*Champsosaurus*	*albertensis*	RTMP 86.12.11
		Champsosaurus	*ambulator*	AMNH 983
		Champsosaurus	*dolloi*	IRSNB 3662, 1582, 58480
		Champsosaurus	*gigas*	SMM P 77.33.24
		Champsosaurus	*laramiensis*	AMNH 982
		Champsosaurus	*natator*	NMC 8919
	Short	*Simoedosaurus*	*dakotensis*	SMM P 76.10.1
		Simoedosaurus	*lemoinei*	MNHN BL 1878, 2916, 9401, 9421, 9401, 9425, 9700, 10416, 11093, 12064, 14637, 16818; BR 9395, 13806
Crocodylia	Long	*Gavialis*	*gangeticus*	KPM-NFR 17 (G1), 18 (G2), 52 (G3), 55 (G4), 92 (G5)
		Tomistoma	*schlegelii*	KPM-NFR 64 (T1); UMUT 12279 (T2); UMZC R 5842 (T3)
	Long & wide	*Crocodylus*	*acutus*	UMZC R 6051 (Cra)
	Short/ medium	*Alligator*	*mississippiensis*	KPM-NFR 16 (A1), 109 (A2); UMZC R 6301 (A3)
		Alligator	*sinensis*	UMUT 12252 (As)
		Caiman	*crocodilus*	NSM-PO 421 (Cc1), 425 (Cc2)
		Caiman	*latirostris*	KPM-NFR 54 (Cla1), 84 (Cla2)
		Paleosuchus	*palpebrosus*	UMUT 13041 (P)
		Crocodylus	*niloticus*	UMUT 12260 (Cn)
		Osteolaemus	*tetraspis*	KPM-NFR 110 (O)

Table S1. List of choristoderan and extant crocodilian specimens used in this study.

species	posture	v2/v3	v3/v4	v4/v5	v5/v6	v6/v7	v7/v8	v8/v9
Gavialis gangeticus								
torsion	st	**3.23°**	-2.28°	**2.58°**	-0.42°	0.88°	-0.34°	1.13°
	up	1.04°	-0.62°	1.02°	-0.67°	1.54°	-0.35°	1.31°
	lat	-2.52°	**-5.45°**	-1.15°	-2.22°	-0.49°	0.66°	1.84°
dorsi-flex (θ°)	st (θ_{st})	-9.01°	10.04°	8.01°	2.33°	1.21°	5.67°	8.75°
	up (θ_{up})	3.54°	**21.42°**	**15.34°**	5.26°	2.14°	6.09°	6.75°
	lat (θ_{lat})	-5.10°	8.46°	14.94°	**15.98°**	7.21°	5.75°	5.79°
lateral flex (ϕ°)	st (ϕ_{st})	0.71°	8.08°	**-10.08°**	-6.36°	-0.39°	2.06°	4.05°
	up (ϕ_{up})	-1.56°	-0.78°	-7.33°	-5.23°	-3.31°	2.69°	7.38°
	lat (ϕ_{lat})	**17.88°**	**21.33°**	2.92°	-1.26°	-1.51°	5.73°	8.57°
Caiman latirostris								
torsion	st	-0.21°	-1.92°	-1.35°	0.58°	0.98°	-1.46°	-1.65°
	up	0.42°	-2.16°	-0.98°	1.83°	-0.35°	-1.86°	**-3.07°**
	lat	-1.32°	-1.83°	**-2.97°**	0.60°	**2.45°**	1.29°	0.85°
dorsi-flex (θ°)	st (θ_{st})	1.09°	-3.91°	2.12°	0.27°	8.25°	6.92°	11.96°
	up (θ_{up})	0.88°	5.57°	16.68°	**17.72°**	**20.11°**	**19.20°**	16.00°
	lat (θ_{lat})	0.45°	-0.35°	6.29°	6.69°	16.26°	13.89°	17.16°
lateral flex (ϕ°)	st (ϕ_{st})	-0.50°	-2.24°	-1.47°	2.59°	1.50°	0.55°	-1.21°
	up (ϕ_{up})	0.43°	-0.65°	-2.14°	0.58°	-4.29°	-7.89°	-12.13°
	lat (ϕ_{lat})	7.88°	14.31°	13.88°	**20.19°**	**15.62°**	**15.54°**	8.78°

Table S2. The angles of inter-cervical torsion, dorsi-flexion (θ°), and lateral flexion (ϕ°) angles *in vivo* measured for *Gavialis gangeticus* (KPM-NFR 52) and *Caiman latirostris* (KPM-NFR 54) specimens CT-scanned in the Straight (st), Upward (up), and Laterally-flexed (lat) neck postures.

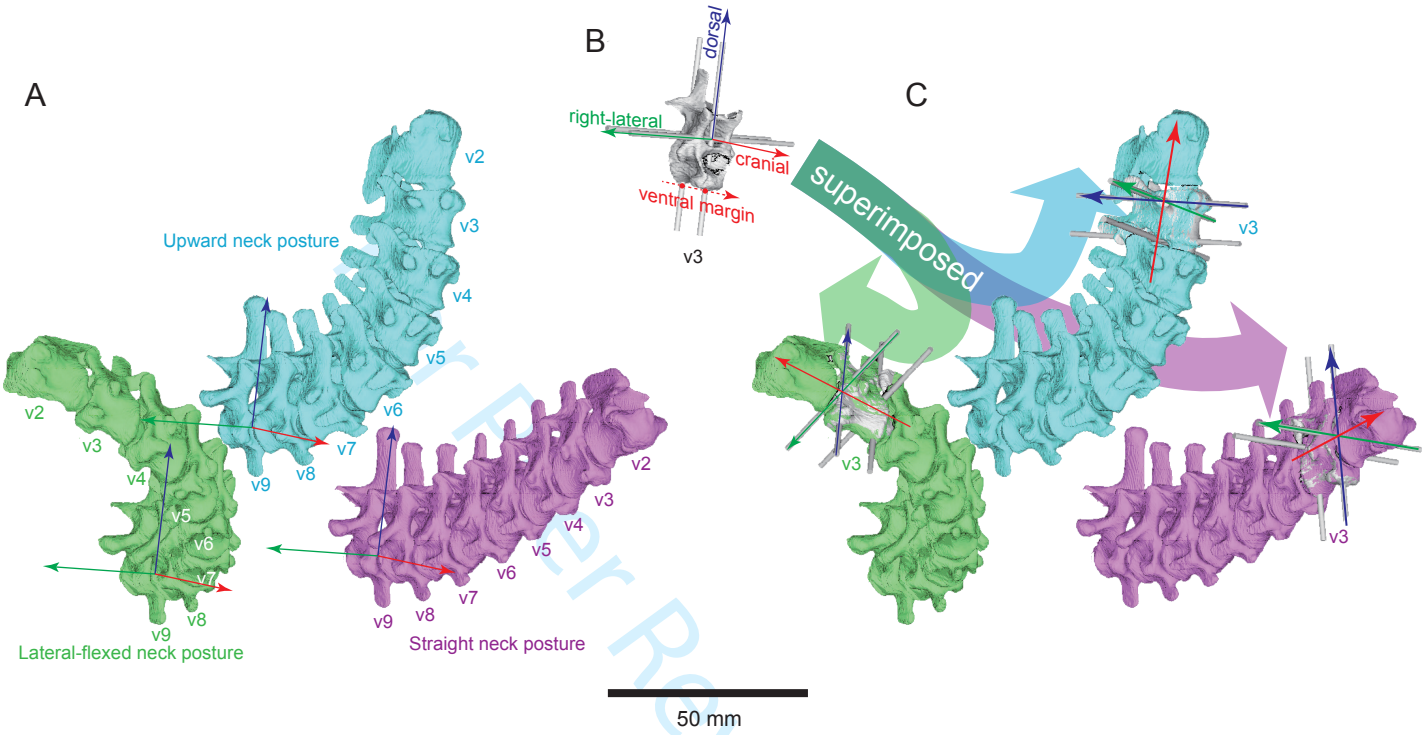

Supp. Fig. S1 Methodology used to measure the orientation of each cervical element in *Caiman latirostris* (KPM-NFR 54); A, cervical vertebrae (v2–9) in three different neck postures (Straight, Upward, and Lateral-flexed) are shown. The arrows in "A" indicate the unit-vectors of cranio-caudal (red), dorso-ventral (blue), and medio-lateral (green) axes of the ninth cervical (v9); B, an isolated cervical vertebra (e.g., third cervical [v3]) is labelled with the three unit-vectors; and C, the vertebra with the unit-vectors (e.g., v3) was superimposed onto its relevant in situ position in the neck for the three different neck postures, respectively. The inter-cervical joint angles were estimated using the unit-vectors of each consecutive pair of cervical vertebrae.

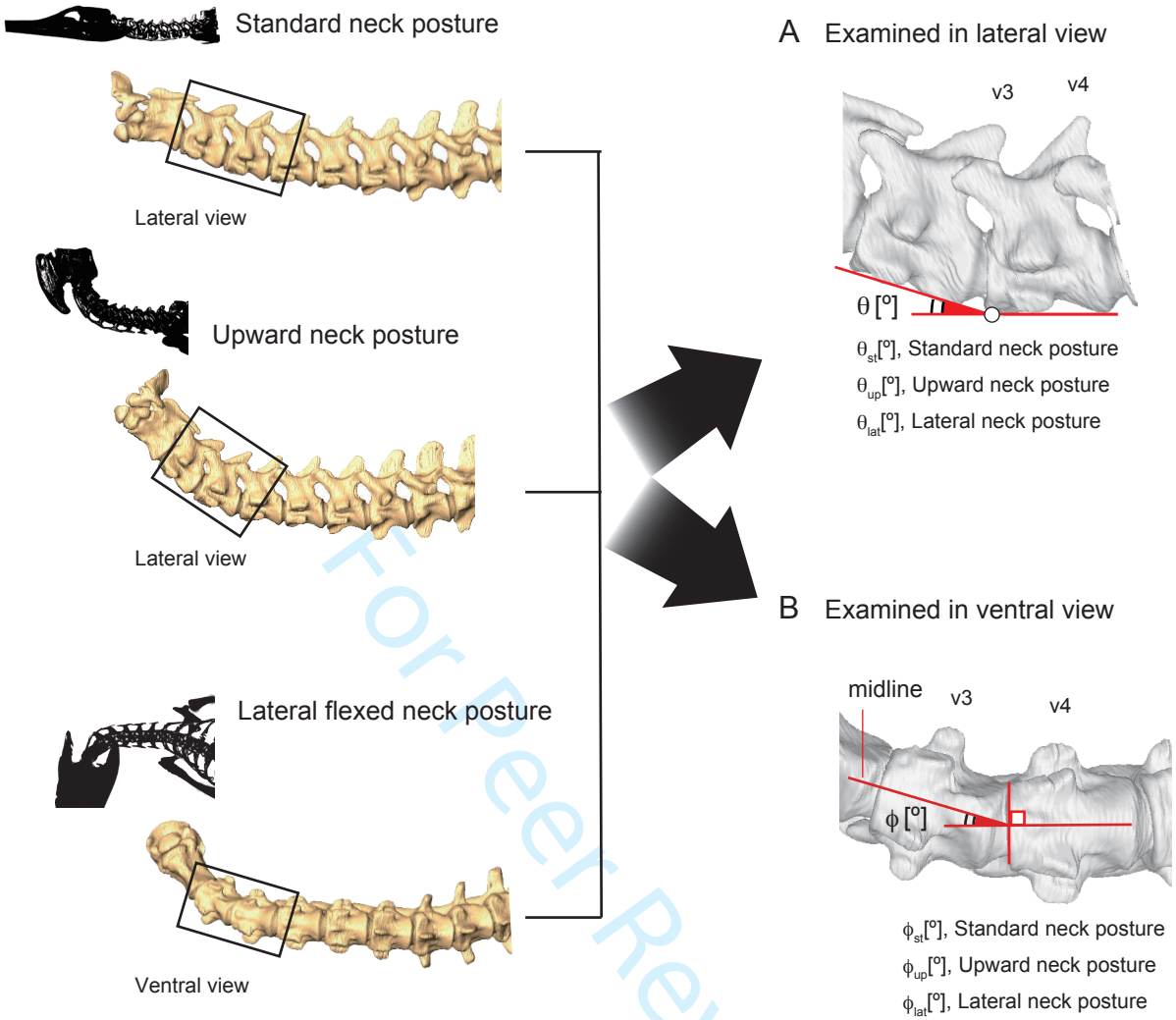

Supp. Fig. S2 Inter-cervical articulation angles in situ taken from fresh specimens of *Gavialis gangeticus* used for validation. Standard and Upward neck postures examined in left lateral view (A); Lateral-flexed neck posture examined in ventral view (B). The same method was used for *Caiman latirostris*.

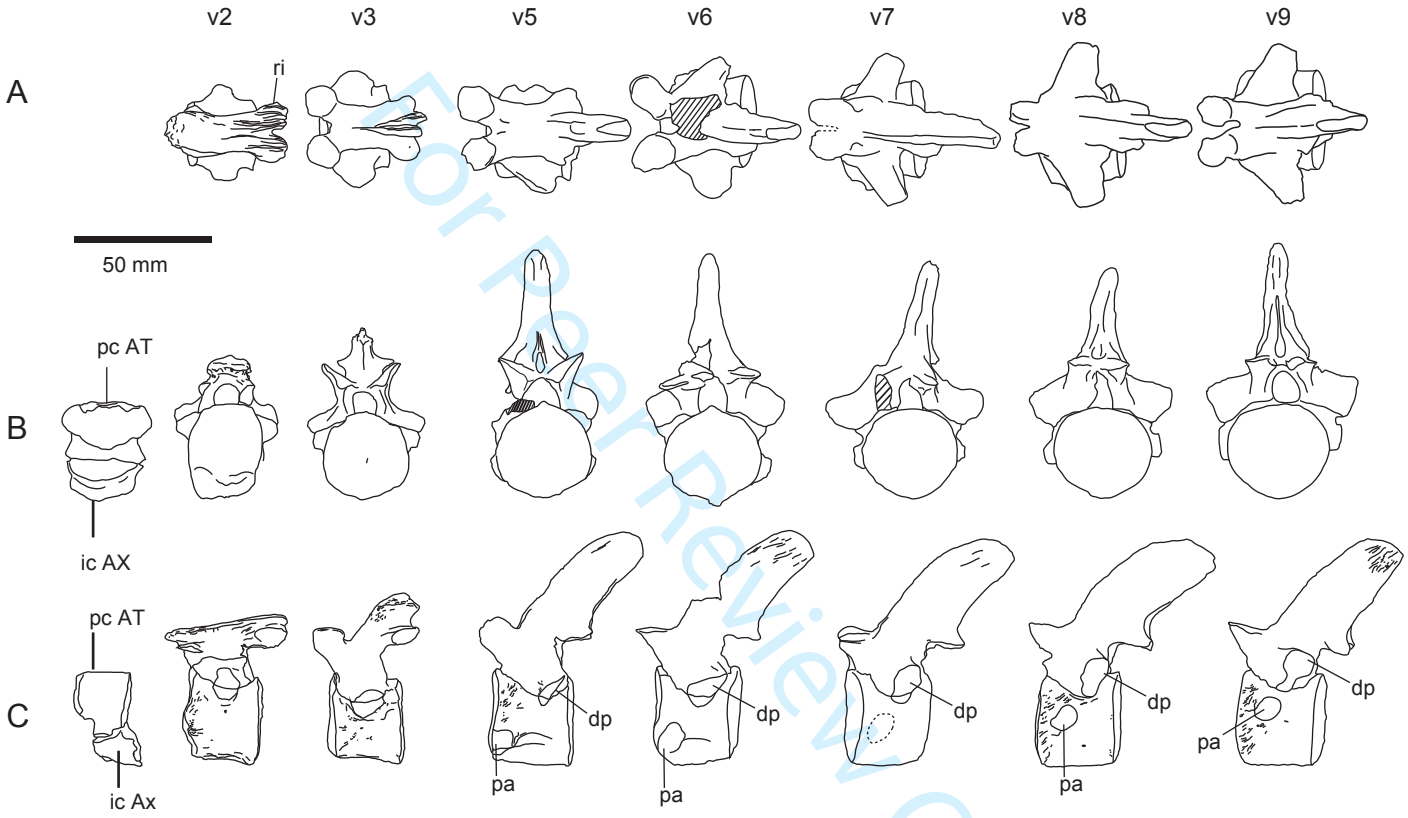

Supp. Fig. S3 *Champsosaurus gigas* (SMM P 77.33.24) cervical vertebrae v1–9: A, in dorsal; B, in anterior; C, in left lateral views. Abbreviations: pc AT, pleurocentrum of atlas; ic AX, inter-centrum of axis; dp, diapophysis; pa, parapophysis; ri, ridge.

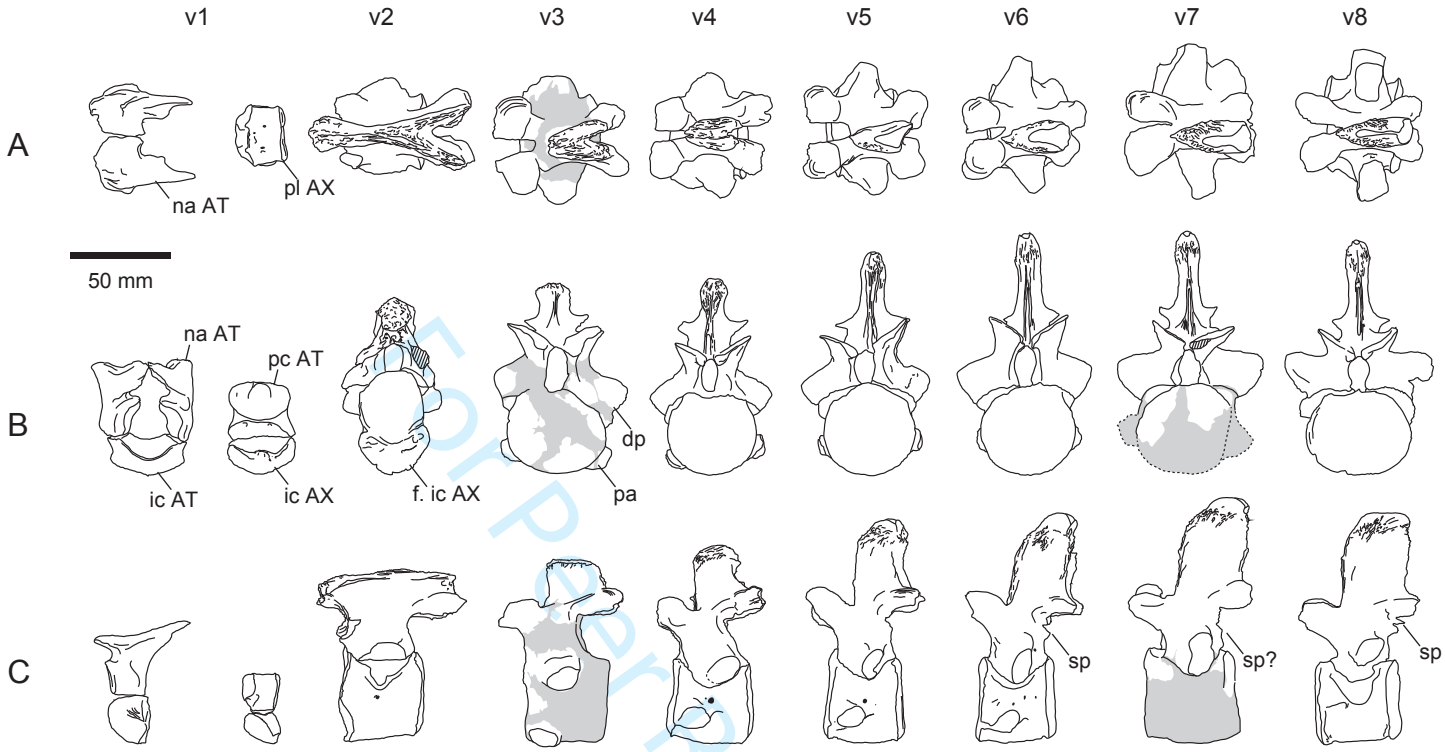

Supp. Fig. S4 *Simoedosaurus dakotensis* (SMM P 76.10.1) cervical vertebrae v1–8: A, in dorsal; B, in anterior; C, in lateral views. Abbreviations: dp diapophysis; f. ic AX; facet for inter-centrum of axis; ic AT, inter-centrum of atlas; ic AX, inter-centrum of axis; na AT, neural arch of atlas; pa, parapophysis; pl AX, pleurocentrum of axis; sp, spinous process.

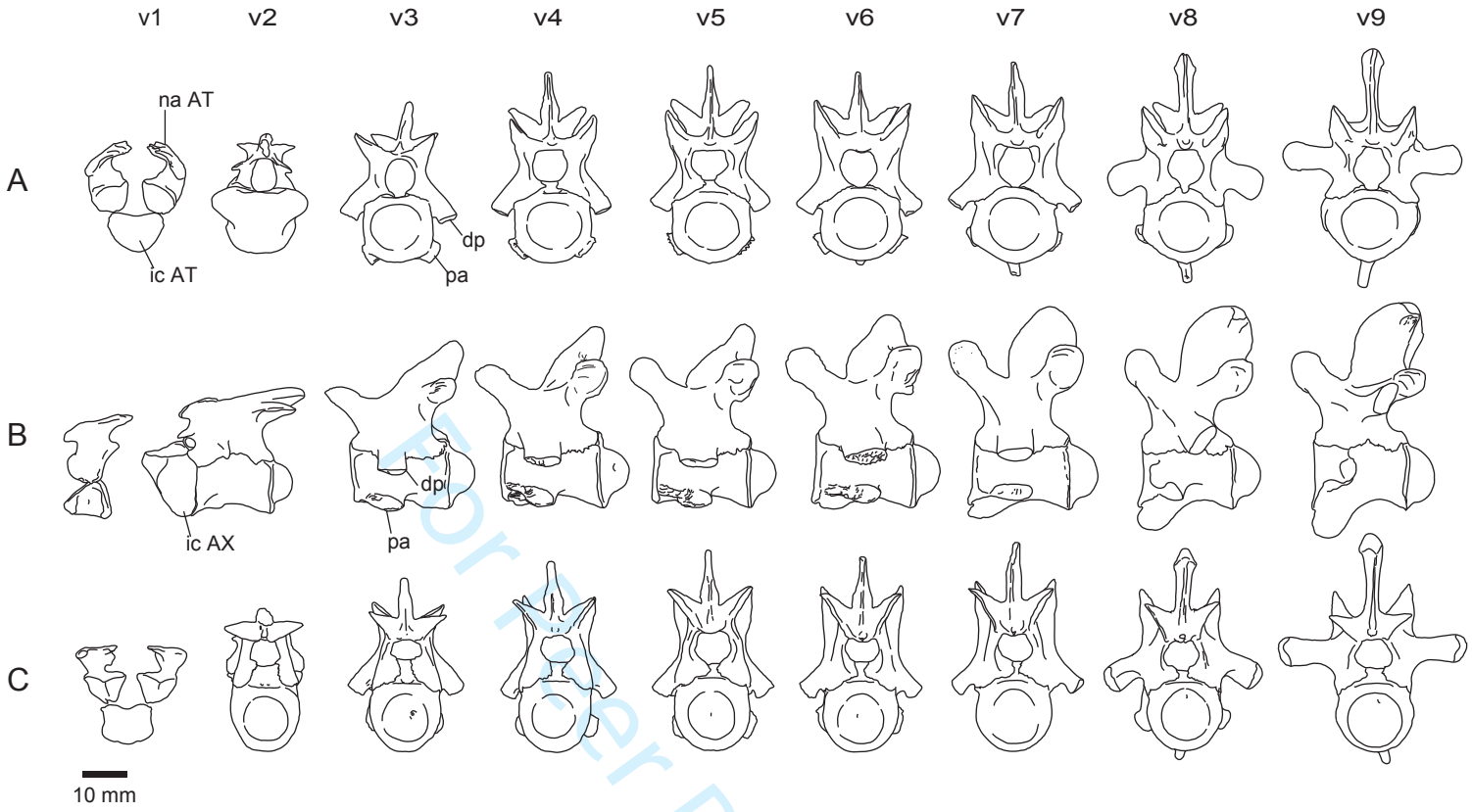

Supp. Fig. S5 *Gavialis gangeticus* (KPM-NFR 18) cervical vertebrae v1–9; A, in anterior; B, in left lateral; C, in posterior views. Abbreviations are the same as in Figure S4.

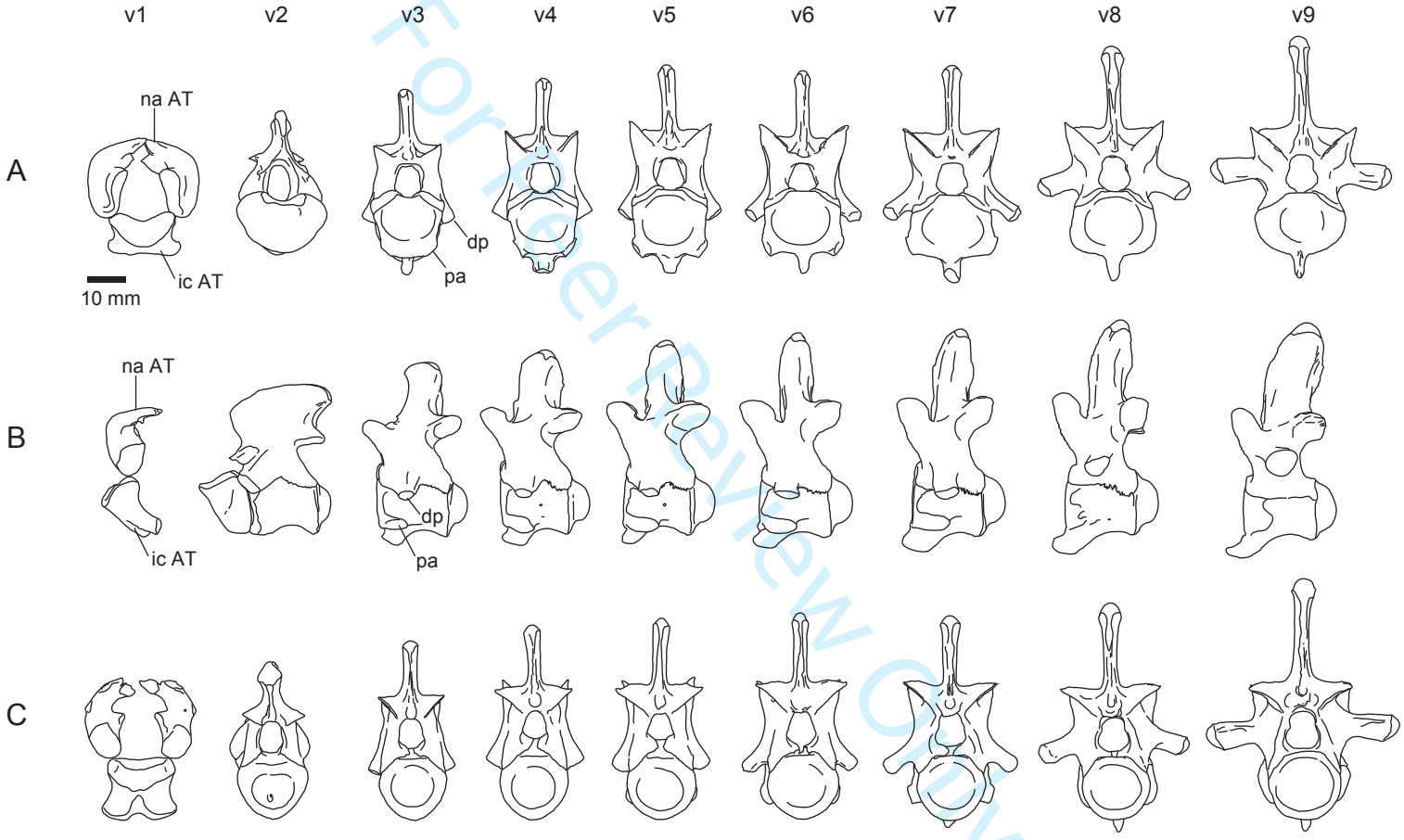

Supp. Fig. S6 *Alligator mississippiensis* (KPM-NFR 16) cervical vertebrae v1–9; A, in anterior; B, in left lateral; C, in posterior views. Abbreviations are the same as in Figure S3.

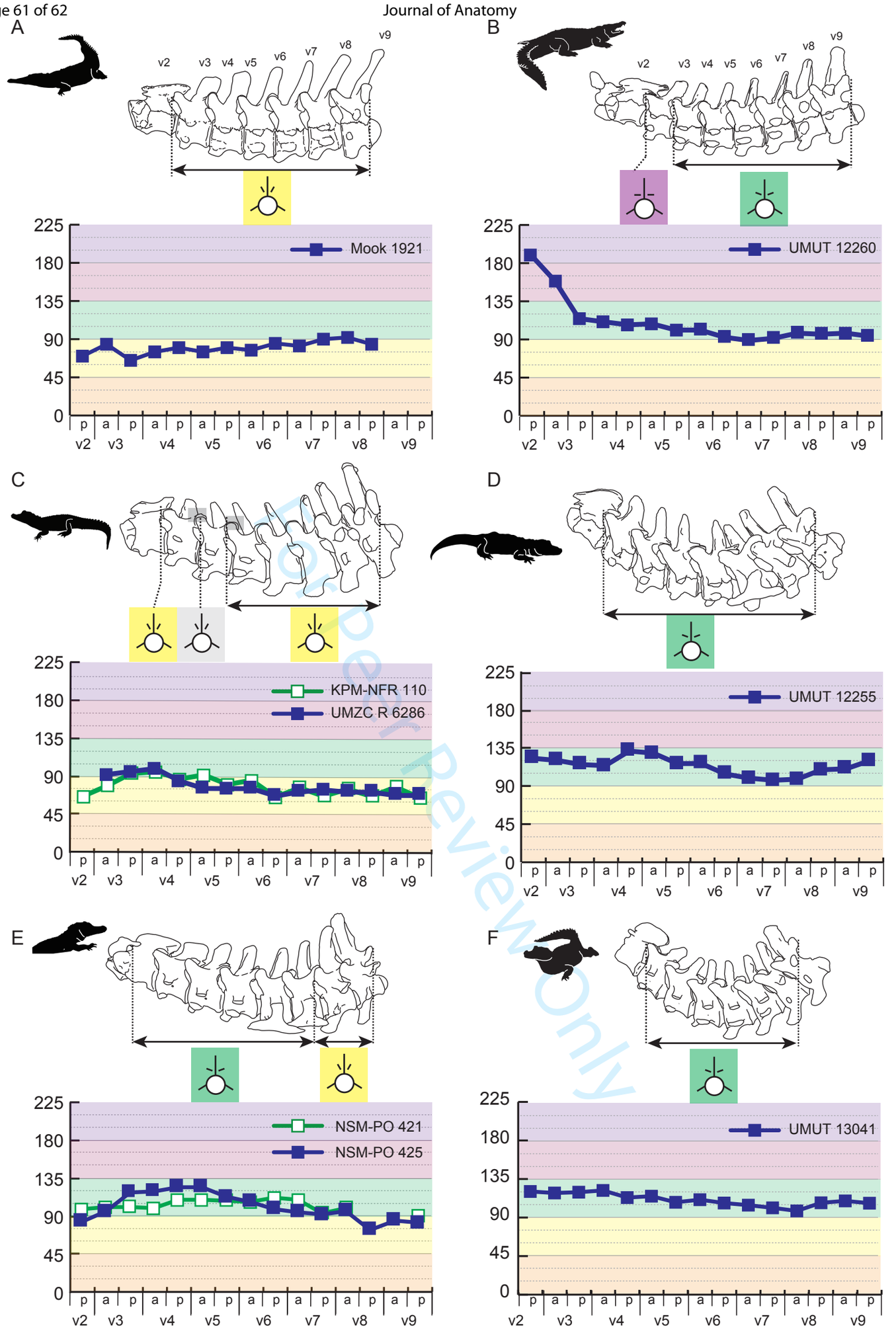

Supp. Fig. S7 Positional change of the Enclosed zygapophysial angles (EZA) in Crocodylia. The diagram shows positional changes in EZA along the neck (v2–9) for each taxon. A, *Crocodylus acutus* (Mook, 1921); B, *Crocodylus niloticus* (UMUT 12260); C, *Osteolaemus tetraspis* (KPM-NFR 110; UMZC R 6286); D, *Alligator sinensis* (UMUT 12255); E, *Caiman crocodilus* (NSM-PO 421, 425); F, *Paleosuchus palpebrosus* (UMUT 13041).

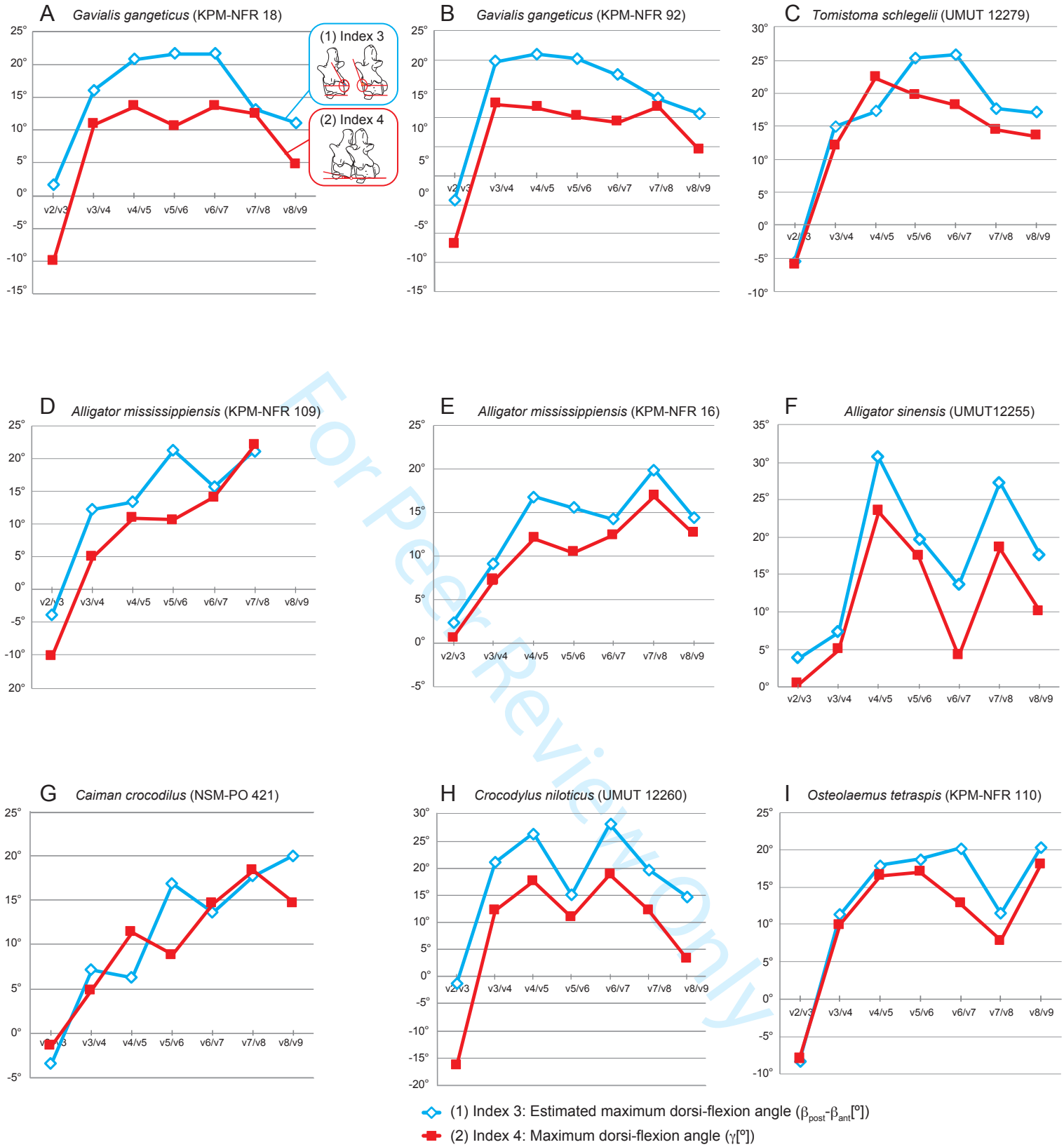

Supp. Fig. S8 Angle of inter-cervical dorsi-flexion of v2–9, estimated from Indices 3 (βpost°-βant°) and 4 (γ°); A, *Gavialis gangeticus* (KPM-NFR 18); B, *Gavialis gangeticus* (KPM-NFR 92); C, *Tomistoma schlegelii* (UMUT 12779); D, *Alligator mississippiensis* (KPM-NFR 109); E, *Alligator mississippiensis* (KPM-NFR 16); F, *Alligator sinensis* (UMUT 12255); G, *Caiman crocodilus* (NSM-PO 421); H, *Crocodylus niloticus* (UMUT 12260); I, *Osteolaemus tetraspis* (KPM-NFR 110); J, *Paleosuchus palpebrosus* (UMUT 13041).